JAERI-M
93-219

AN INVESTIGATION OF A.C. LOSSES IN TWO SUB-SIZE CONDUCTORS FOR THE ITER

November 1993

Richard J. NELSON*, Yoshikazu TAKAHASHI
Takaaki ISONO, Tomoyuki SASAKI
Kiichi OHTSU and Fumio TAJIRI

日本原子力研究所
Japan Atomic Energy Research Institute

JAERI-Mレポートは，日本原子力研究所が不定期に公刊している研究報告書です。
入手の問合わせは，日本原子力研究所技術情報部情報資料課（〒319－11茨城県那珂郡東海村）あて，お申しこしください。なお，このほかに財団法人原子力弘済会資料センター（〒319-11茨城県那珂郡東海村日本原子力研究所内）で複写による実費頒布をおこなっております。

JAERI-M reports are issued irregularly.
Inquiries about availability of the reports should be addressed to Information Division, Department of Technical Information, Japan Atomic Energy Research Institute, Tokai-mura, Naka-gun, Ibaraki-ken 319-11, Japan.

編集兼発行　日本原子力研究所
印　　刷　日立高速印刷株式会社

JAERI-M 93-219

An Investigation of A.C. Losses in Two Sub-size Conductors for the ITER

Richard J. NELSON*, Yoshikazu TAKAHASHI, Takaaki ISONO
Tomoyuki SASAKI, Kiichi OHTSU and Fumio TAJIRI

Department of Fusion Engineering Research
Naka Fusion Research Establishment
Japan Atomic Energy Research Institute
Naka-machi, Naka-gun, Ibaraki-ken

(Received October 12, 1993)

Two second sub-size CiC conductors manufactured as models for the full-size conductors to be used in the polodial coils of the ITER tokamak machine were tested to determine their A.C. loss characteristics. One conductor was manufactured by Furukawa (a 3x4x4 strand conductor), the other by Hitachi Cable (3x3x3). Each sub-size conductor sample, wound in a solenoid, was tested in a background magnet with zero transport current. For a single cycle ramp-up from 0 T to 1.15 T and then back to zero, hysteresis loss for the Furukawa conductor was 12.6 mJ per cubic centimeter of conductor volume (not including conduit), while the hysteresis loss for the Hitachi Cable sample was 19.9 mJ/cc. Each sample was then forced to experience an exponential decay of the background field, using different decay time constants for each trial, and the coupling loss was subsequently plotted versus the inverse of the background field decay. A "best-estimate" value for the coupling time constant for each sample was determined based on theory; the Furukawa sample had a coupling time constant of about 27(±5) ms, while the Hitachi Cable sample had a coupling time constant of about 11(±5) ms.

---

* Massachusetts Institute of Technology

JAERI-M 93-219

ITER超電導コイル用縮小導体の交流損失の測定

日本原子力研究所那珂研究所核融合工学部
Richard J. NELSON*・高橋　良和・磯野　高明
佐々木知之・大都　起一・田尻二三男

（1993年10月12日受理）

ITERトカマク装置のポロイダル・コイルに用いられる超電導導体の縮小モデルとして製作された2種類の縮小ケーブル・イン・コンジット導体の交流損失を測定した。2種類の導体は，古河電気工業㈱（素線：3×4×4本）及び日立電線㈱（素線：3×3×3本）によって製作された。これらの導体は，ソレノイド状に巻線され，通電電流なしで，バックグランド磁場コイルの中で実験された。ヒステリシス損失は，0Tから1.15Tまでバックグランド磁場を上下さして，測定された。その結果，ヒシテリシス損失の測定値は，それぞれ12.6mJ／cc（古河）及び19.9mJ／cc（日立）であった。ただし，これらのCCにはコンジットの体積を含まない。これらの値は，それぞれの素線の測定結果と一致した。カップリング損失は，バックグランド磁場を一定の値から指数関数型に減衰させ，その時定数をパラメータにして測定された。測定されたカップリング損失の時定数は，それぞれ，27（±5）ms（古河）及び11（±5）ms（日立）であった。これらの値は，素線の計算値の約10倍である。これについては，今後も検討を行い，最適化する必要がある。

那珂研究所：〒311－01 茨城県那珂郡那珂町大字向山801－1
＊　マサチュセッツ工科大学

Contents

目　　次

NOMENCLATURE

a	Signal amplifier value
A_{cpl}	Area on the M-H plot corresponding to coupling loss [V^2s]
A_{hys}	Area on the M-H plot corresponding to hysteresis loss [V^2s]
A_{hys+}	An area on the M-H plot [V^2s]
A_i	Area enclosed by the inner pick-up coil [m^2]
A_m	Effective cross-sectional area of magnetized material [m^2]
A_{non}	An area on the M-H plot [V^2s]
A_o	Area enclosed by the outer pick-up coil [m^2]
A_{xtr}	An area on the M-H plot [V^2s]
$A_{z,actual}$	Cross-sectional area of actual conductor when cut parallel to the z-axis [m^2]
$A_{z,model}$	Cross-sectional area of model slab when cut parallel to the z-axis [m^2]
B_e	External magnetic flux density (or external magnetic induction) [T]
B_i	Internal magnetic flux density (or internal magnetic induction) [T]
$\dot{B}_i$	Time rate of change of internal magnetic flux density [T/s]
B_{max}	Maximum external magnetic flux density [T]
c	A conversion factor from measured voltage to corresponding magnetic field
d_{es}	Equivalent model slab thickness [m]
d_i	Inner diameter of the conduit [m]
d_o	Outer diameter of the conduit [m]
D_i	Inner diameter of the sample solenoid [m]
E	Electric field [V/m]
H	Magnetic field [A/m]
I_{max}	Maximum current in the background field magnet [A]
J_f	Free current density [A/m^2]
l	Twist Pitch [m]
L	Inductance of the background field magnet (L=0.11 H)
M	Magnetization [T]
M_{int}	Area on the M-H curve integrated by the computer program "LOSS" [V^2s]
M_{top}	Magnetization when the background field magnet carries I_{max} [Vs]
μ_0	Magnetic permeability ($\mu_0=4\pi x10^{-7}$ H/m)
N	Number of turns on a coil

1. INTRODUCTION

A.C. Losses affect every superconducting magnet that must experience changing magnetic fields. These energy losses may jeopardize the reliability (and even safety) of a superconducting magnet system: the quench of the superconducting polodial magnet in a large tokamak fusion reactor, for example, would be an enormous inconvenience if not a serious safety hazard. It is therefore convenient to minimize the A.C. losses of the conductor, since they cannot be completely eliminated. To this end, tests have been previously designed to measure A.C. losses.

This report gives the test results of A.C. loss measurements of two sub-size, cable-in-conduit conductors (one manufactured by Furukawa, the other by Hitachi Cable); they are the small-scale samples of full-size conductors intended for use in the polodial coils of the ITER tokamak fusion machine. The A.C. loss tests were performed at the Japan Atomic Energy Research Institute (JAERI) on June 16-18, 1993.

1.1 Sample Specifications

The two samples used in the A.C. loss experiment were both cable-in-conduit conductors wound into solenoids. One conductor was manufactured by the Furukawa Electric Co., Ltd. and the other by Hitachi Cable, Ltd. In each case the strands were made using a bronze process, coated with chrome and then twisted. The twisting was performed in three stages, yielding a 3x4x4=48 strand Furukawa conductor and a 3x3x3=27 strand Hitachi conductor. At each cabling stage the strand groups were twisted in the same direction (a right-handed curl with the thumb in the direction of current). The conductors were then wrapped with 25 mm wide stainless steel tape and inserted into round cross-section titanium conduits.

The following table presents the major parameters of the test samples.

Table 1.

Manufacturer:	Furukawa	Hitachi Cable
Superconducting Material:	$(NbTi)_3Sn$	$(NbTi)_3Sn$
Strand Stabilizer Material:	Oxygen-Free Cu	Oxygen-Free Cu
Strand Barrier Material:	Ta	Ta
Strand Coating Material:	Cr	Cr
Strand Outside Diameter:	0.920 mm	0.923 mm
Strand Core Diameter:	0.564 mm	0.587 mm
Filament Diameter:	2 μm	2.44 μm
Number of Filaments (per strand):	19 x 1189 = 22,591	121 x 121 = 14,641
Filament Twist Pitch:	20 mm	21.2 mm
Barrier Thickness:	10 μm	9.9 μm
Coating Thickness:	2 μm	2.3 μm
Copper Ratio:	1.58	1.47
Conduit Material:	Ti	Ti
Number of Strands in Conductor:	3 x 4 x 4 = 48	3 x 3 x 3 = 27
Void Fraction:	35%	37%
Conduit Outside Diameter:	9.84 mm	8.4 mm
Conduit Inside Diameter:	8.06 mm	6.0 mm
Cabling Twist Pitch (3 stages):	110 mm/180 mm/330 mm	82 mm/130 mm/250 mm
Inside Diameter of Solenoid Windings:	101.6 mm	100.0 mm
Number of Turns on the Solenoid:	12	13
Diameter of Inner Pick-up Coil:	97 mm	97 mm
Number of Turns on Inner Pick-up Coil:	60	65
Diameter of Outer Pick-up Coil:	121.3 mm	119 mm
Number of Turns on Outer Pick-up Coil:	34	36

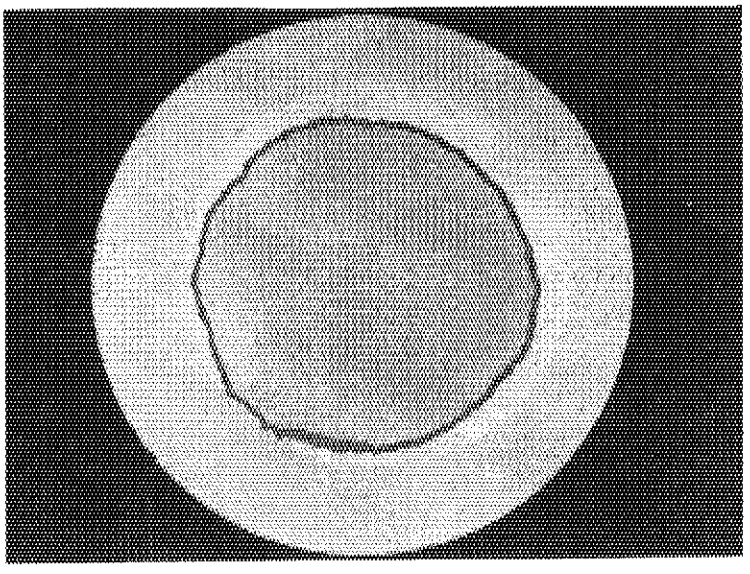

Photo 1 A view of the cross-section of a single strand of the Furukawa conductor. The central region contains 22,591 Nb_3Sn filaments with niobium and bronze, surrounded by a tantalum barrier (the dark region). Outside the barrier is the copper stabilizer, with a thin layer of chromium on the strand surface.

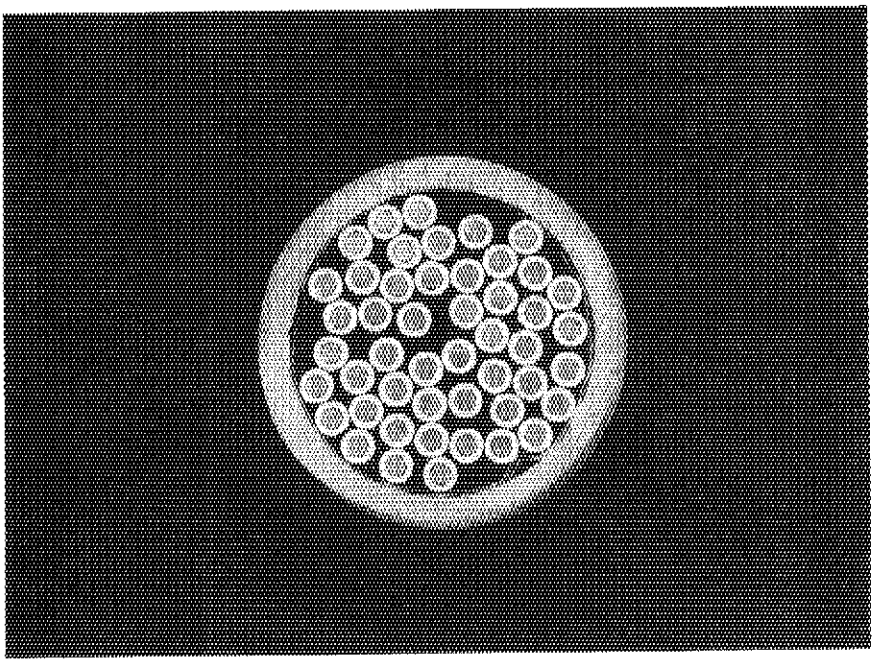

Photo 2 A view of the cross-section of the Furukawa sub-size (3x4x4) cable-in-conduit conductor.

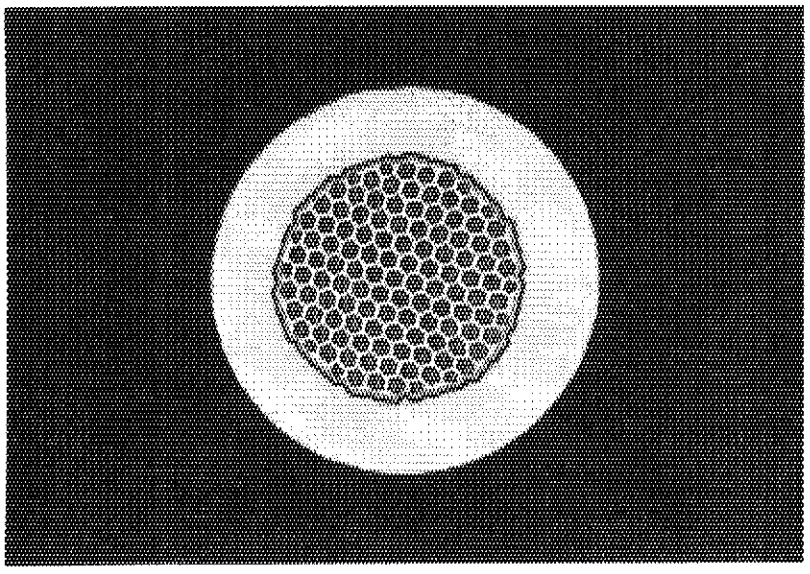

Photo 3 A view of the cross-section of a single strand of the Hitachi conductor. In the central region, each of the 121 hexagonal elements contains 121 Nb_3Sn filaments (for a total of 14,641 filaments per strand). Niobium and bronze are also present in the central region, surrounded by a tantalum barrier, copper stabilizer, and a thin coating of chromium.

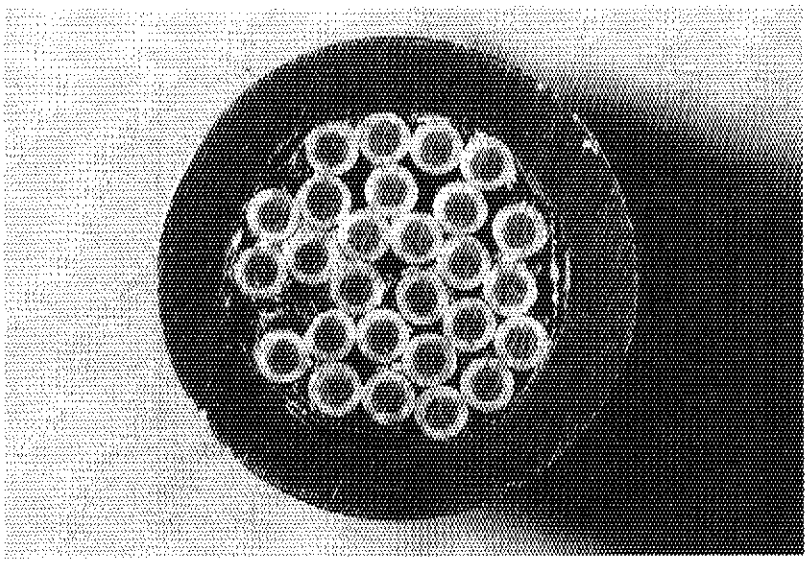

Photo 4 A view of the cross-section of the Hitachi sub-size (3x3x3) cable-in-conduit conductor.

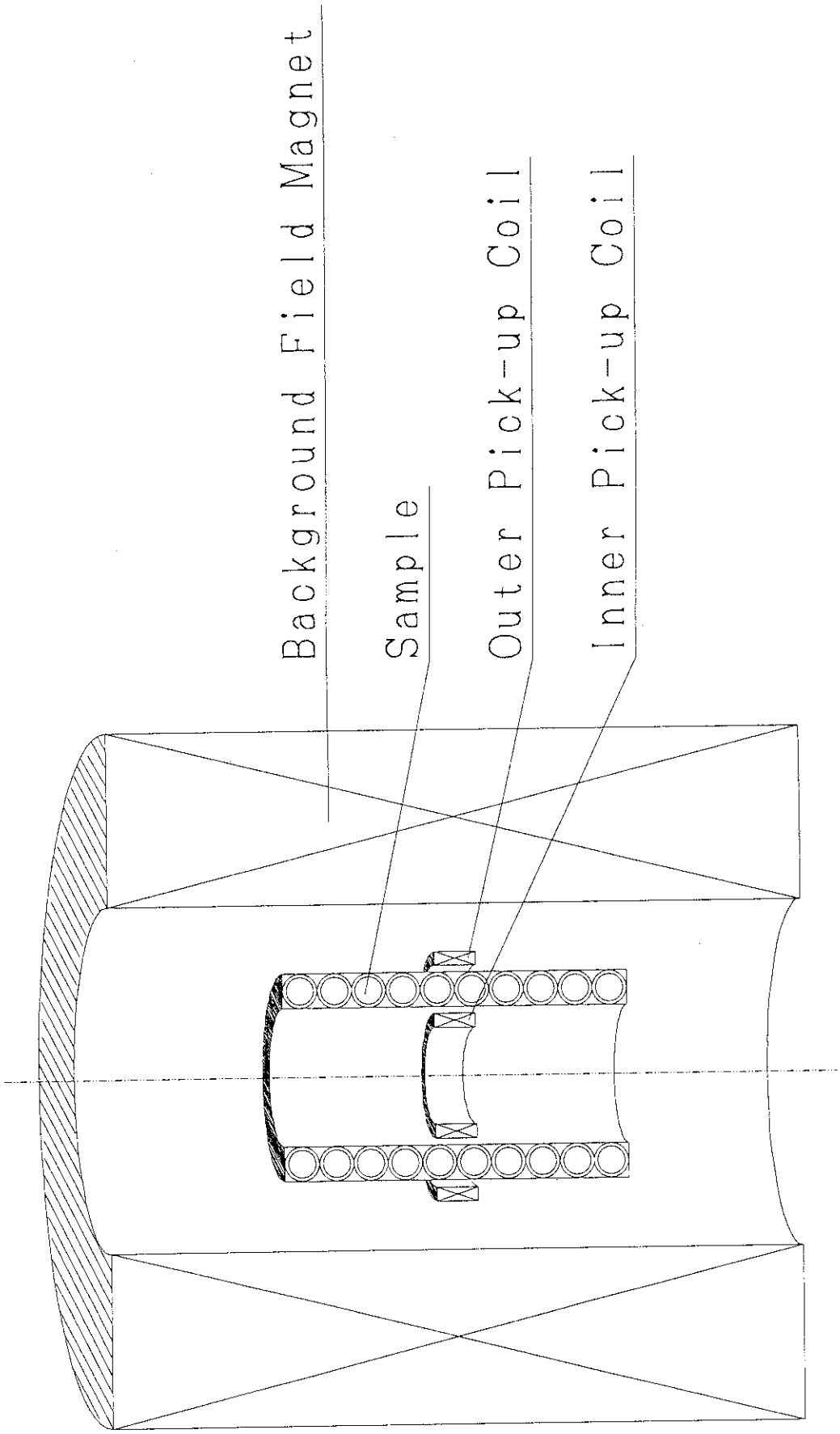

Fig. 1 Cross-sectional cut showing the relative locations of the experimental coil and pick-up coils. Not to scale.

1.2 Experimental Setup

The sample solenoid, with its inner and outer pick-up coils, was placed in the background field magnet, as shown in fig. 1. After the magnet and sample were placed in the cryostat where all could be cooled by boiling liquid helium, the instrumentation was assembled: (1) the voltage across a resistor in series with the background field magnet--called the "measurement resistor"--was connected to channel one of the digital memory; (2) the pick-up coil signal was connected to a signal amplifier, and then to channel two of the digital memory. A schematic of the experimental setup is shown in fig. 2.

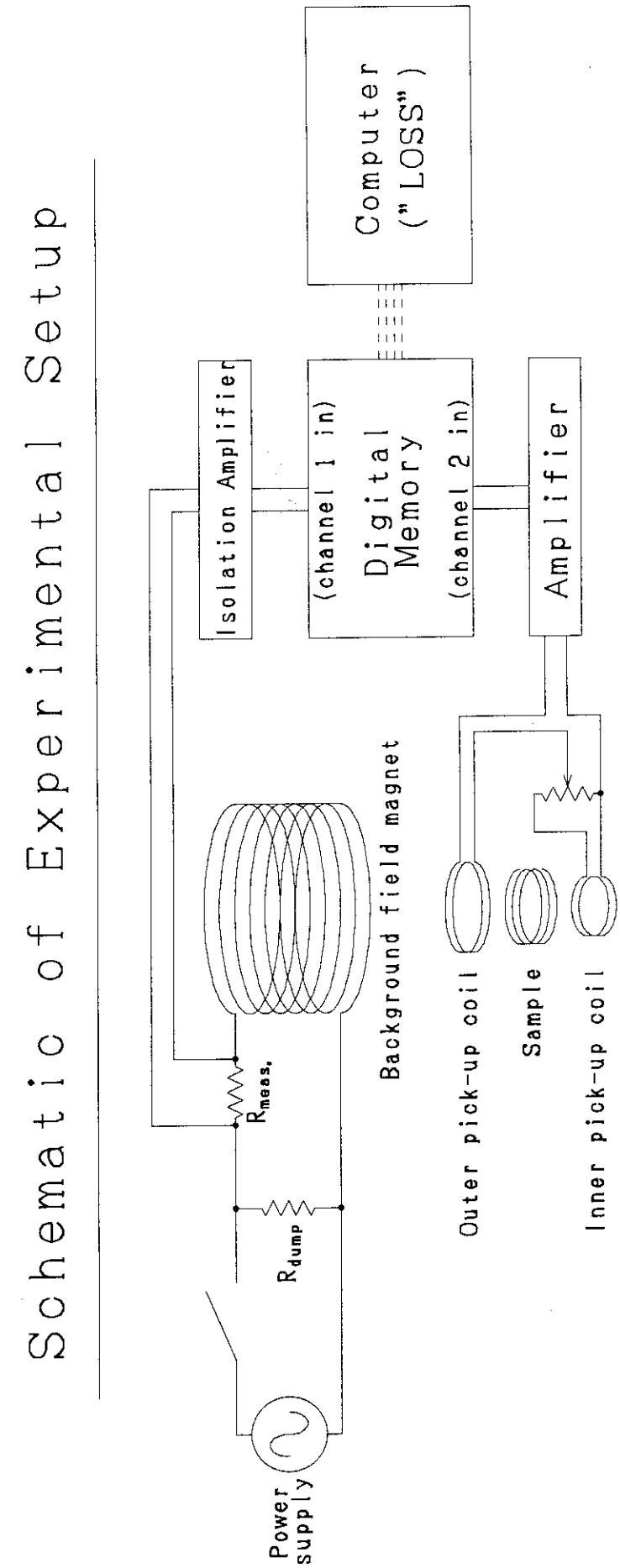

Fig. 2 Schematic of the experimental setup showing the principal instrumentation.

2. THEORETICAL BACKGROUND

2.1 A.C. Losses

The theory behind A.C. Losses has been extensively established in numerous places, hence only an outline relevant to this experiment is given here. From Maxwell's equations, taken in the magnetoquasistatic (MQS) limit, we can easily derive:

$$-\vec{\nabla}\cdot(\vec{E}\times\vec{H}) = \vec{E}\cdot\vec{J}_f + \frac{1}{2}\mu_0\frac{\partial}{\partial t}(H^2) + \vec{H}\cdot\frac{\partial\vec{M}}{\partial t} \tag{1}$$

where J_f is the free current (*not* magnetization current), and the term on the left is the Poynting power supplied to the system. If we integrate this equation over a whole cycle (ramp up and then down), the magnetic energy storage term goes to zero, and we have:

$$Q_{loss} = \oint\vec{E}\cdot\vec{J}_f\,dt + \oint\vec{H}\cdot d\vec{M} \tag{2}$$

where Q_{loss} is the amount of energy dissipated per unit volume. The first term on the right is the ohmic heating due to the transport current which, for this experiment, is zero. Since the magnetization of the sample is diamagnetic, and since we integrate over an entire cycle, we can write the total a.c. losses for the sample as:

$$\begin{aligned} Q_{loss} &= \oint(-M)\,dH \\ &= Q_{hys} + Q_{cpl} \end{aligned} \tag{3}$$

where "hys" and "cpl" stand for "hysteresis" and "coupling", respectively. The hysteresis loss is that portion of the total losses that is independent of the rate of change of external field, while the coupling loss is the "time-dependent" part.

The coupling loss can be theoretically determined assuming the filamentary structure is sufficiently fine for the composite to be treated as a homogeneous mixture; the coupling currents will produce a uniform internal magnetic field B_i given by the solution to [Wilson, pp.176-181]:

$$B_i = B_e - \dot{B}_i\tau_{cpl} \tag{4}$$

where B_e is the external field, and where τ_{cpl}, the coupling time constant of the system, is given in terms of the twist pitch (l) and the effective transverse resistivity of the matrix by:

$$\tau_{cpl} = \frac{\mu_0}{\rho_{et}}\left(\frac{l}{2\pi}\right)^2 \tag{5}$$

In this experiment, the coupling loss calculation was made by an exponentially decaying external field from a maximum field B_{max} to zero with a natural decay constant τ. Using the initial condition $B_i(0)=B_{max}$, we can solve for the internal field as a function of time to find:

$$B_i(t) = \frac{B_{max}}{1-(\tau_{cpl}/\tau)}\left(e^{-t/\tau} - \frac{\tau_{cpl}}{\tau}e^{-t/\tau_{cpl}}\right) \tag{6}$$

The coupling loss can then be calculated as:

$$\begin{aligned} Q_{cpl} &= \int_0^\infty P_{cpl}(t)\,dt \\ &= \int_0^\infty \frac{\dot{B}_i^2}{\rho_{et}}\left(\frac{l}{2\pi}\right)^2 dt = \int_0^\infty \frac{\dot{B}_i^2\tau_{cpl}}{\mu_0}\,dt \\ &= \frac{B_{max}^2}{2\mu_0}\left(\frac{\tau_{cpl}}{\tau + \tau_{cpl}}\right) \end{aligned} \tag{7}$$

2.2 Pick-up Coils

A pick-up coil arrangement is used to measure the magnetization of the sample (see fig. 3). The induced emf around a loop of N turns is:

$$\begin{aligned} V &= N\frac{\partial}{\partial t}\int \vec{B}\cdot d\vec{a} \\ &= N\frac{\partial}{\partial t}\int (\mu_0\vec{H} + \vec{M})\cdot d\vec{a} \end{aligned} \tag{8}$$

The sample to be studied is placed in a magnet that supplies a constant magnetic field

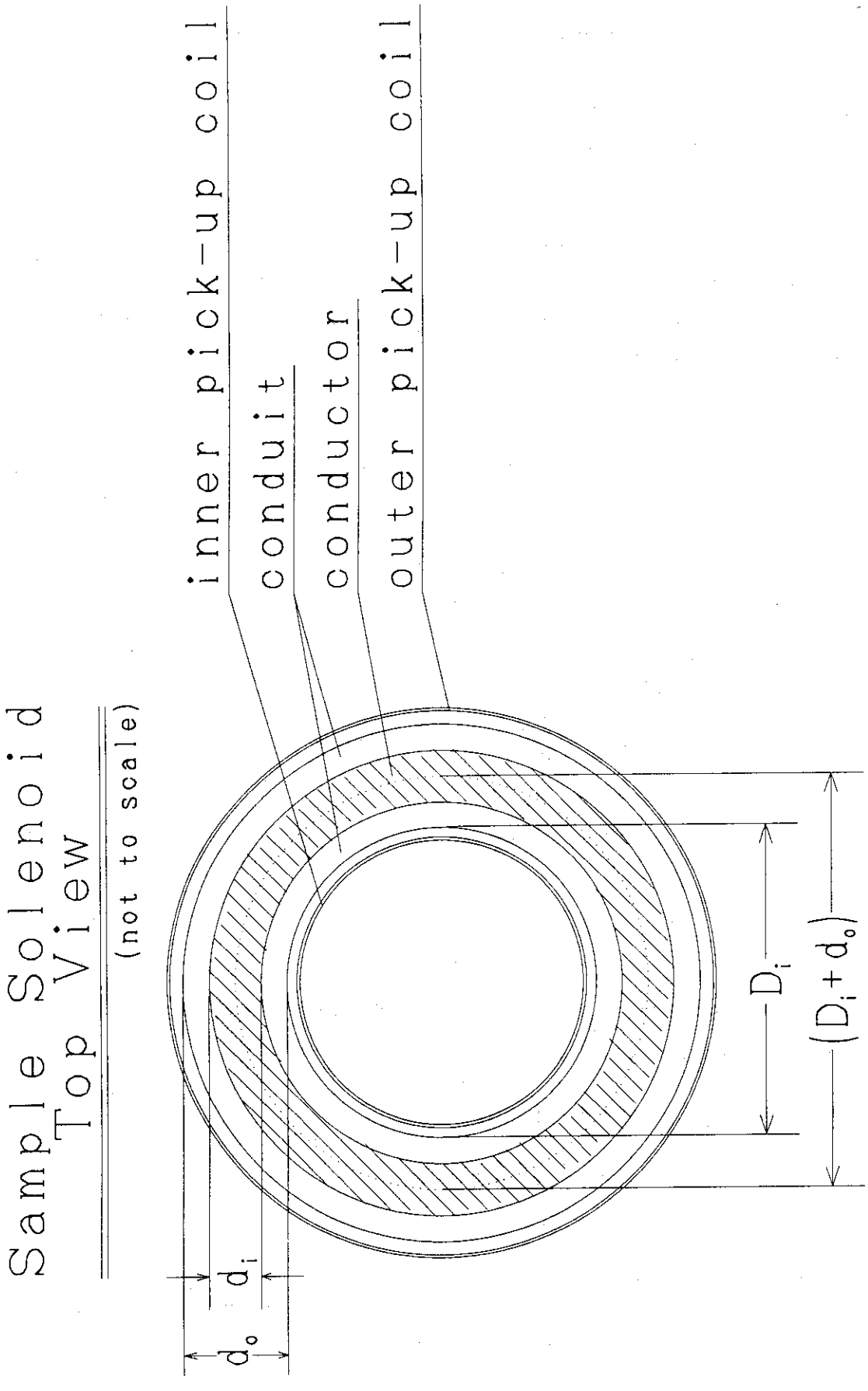

Fig. 3 Top view of the sample with pick-up coils. Not to scale.

over the cross section of the sample; a pick-up coil is located inside the sample, and another outside. In this way, only the outer pick-up coil has its enclosed area pierced by the sample. The induced voltage signal from both of the pick-up coils are then subtracted as follows:

$$\begin{aligned}\Delta V &= V_o - V_i \\ &= \left(N_o \frac{\partial}{\partial t}\int_{A_m} \vec{M}\cdot d\vec{a} + N_o \frac{\partial}{\partial t}\int_{A_o} \mu_0 \vec{H}\cdot d\vec{a}\right) - N_i \frac{\partial}{\partial t}\int_{A_i} \mu_0 \vec{H}\cdot d\vec{a} \\ &= N_o A_m \left(\frac{dM}{dt}\right) + \mu_0 (N_o A_o - N_i A_i)\left(\frac{dH}{dt}\right) \end{aligned} \tag{9}$$

where "o" and "i" designate "outer" and "inner" respectively, and where A_m denotes the cross-sectional area of the magnetized material in the sample. By a judicious choice of number of turns for the pick-up coils (i.e. set $N_oA_o=N_iA_i$), the last term in eq. 9 may be removed, and the magnetization can be easily determined:

$$M = \left(\frac{1}{N_o A_m}\right)\int (\Delta V)\, dt \tag{10}$$

This magnetization is plotted versus the external magnetic field, and integrated numerically to estimate the hysteresis and coupling losses in the sample.

2.3 Physical Model

Because the magnetized material in the sample does not take the form of a uniformly magnetized slab, but rather the circular cross-sections of the filaments and strands, the cross-sectional area of magnetized material seen by the outer pick-up coil (i.e. A_m) is difficult to define. The conductor is therefore modeled as a cylindrical slab (see fig. 4), the model slab and actual conductor having equal volumes; the effective cross-sectional area of magnetized material is defined as the cross-sectional area of the model slab.

We can consider the actual, conduit-wound solenoid and the model cylinder of constant magnetic material thickness both volumes of revolution around the z-axis; the theorem of Pappus allows us to equate the areas of sample cut by a plane through the z-axis, and we get:

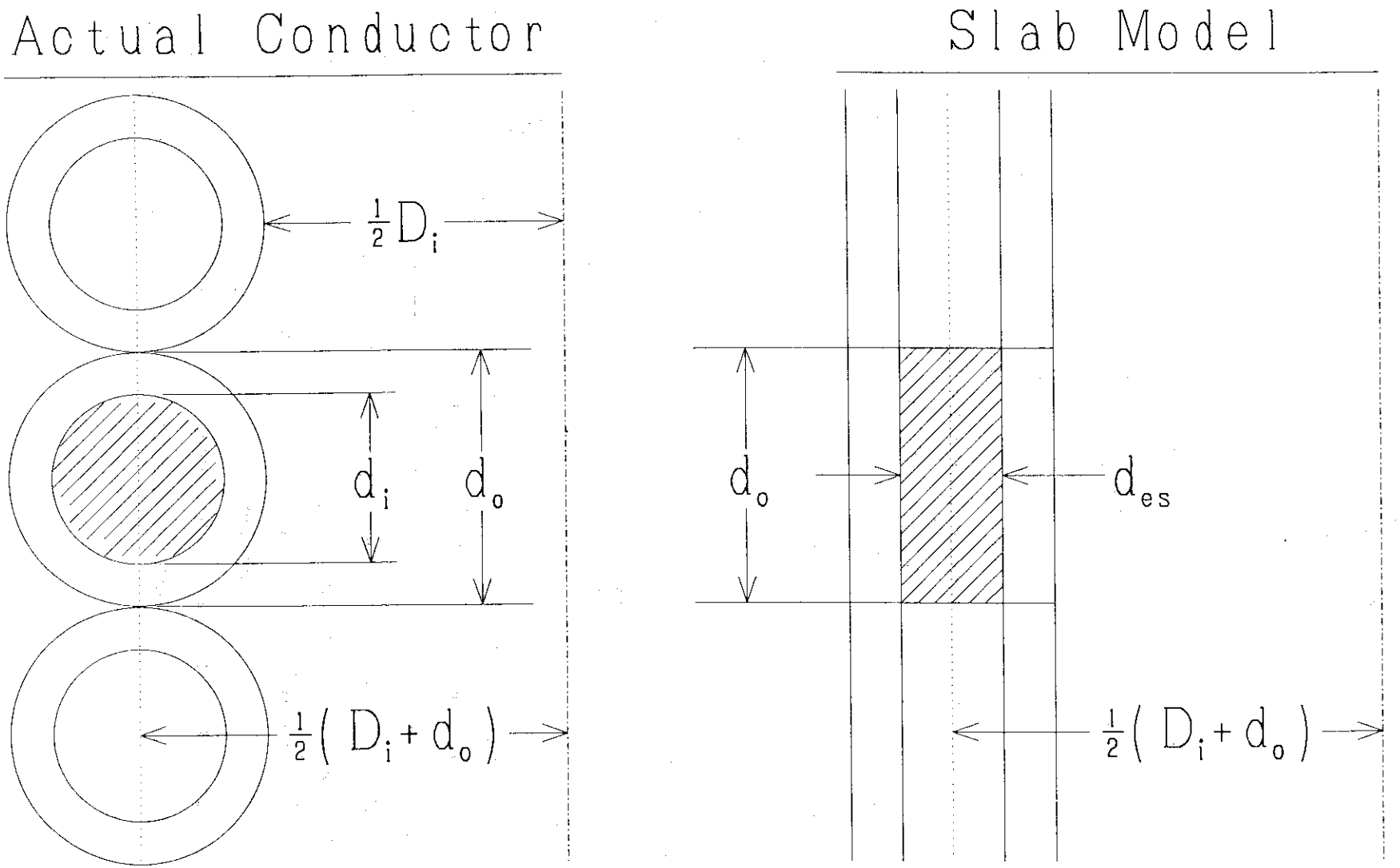

Fig. 4 Cross-sectional view of the actual conductor and the model slab showing the principal dimensions used to calculate the effective magnetized area (A_m) seen by the outer pick-up coil.

$$A_{z,actual} = \frac{\pi}{4} d_i^2$$
$$= d_o d_{es} = A_{z,model} \quad (11)$$

where d_i and d_o are the inner and outer diameters of the actual conduit, respectively, and d_{es} is the effective thickness of the model slab. The effective cross-sectional area as seen by the outer pick-up coil, then, is:

$$A_m = \pi (D_i + d_o) d_{es}$$
$$= \pi (D_i + d_o) \left(\frac{\pi}{4}\right) \frac{d_i^2}{d_o}$$
$$= \left(\frac{\pi d_i}{2}\right)^2 \left(1 + \frac{D_i}{d_o}\right) \quad (12)$$

where D_i is the inner diameter of the sample solenoid. This A_m is the value used to calculate the magnetization in this report.

2.4 Conversion Factors

In this experiment, the magnitude of the background field was determined by measuring the voltage drop (in volts, [V]) across a resistor placed in series with the background magnet (the measurement resistor). In addition, the voltage difference from the pick-up coils (in [V]) was integrated numerically with time by the analysis program "LOSS" before being plotted, and thus the magnetization data carry the unit volts-second, [Vs]. Since "LOSS" then integrated the area under the M-H curve in units of [V^2s], it is convenient to determine the conversion from [V^2s] to a more familiar energy density unit for each sample beforehand.

The resistor used in series with the background magnet was a 2 mΩ resistor, and it was known that a background magnet current of 262 A corresponded to a magnetic induction of 1 T; hence, the conversion from volts to tesla, c=0.524 V/T. Using V_m to represent the voltage across the magnet measurement resistor, and a to represent the signal amplifier for the pick-up coil signal, we can write:

$$Q = \frac{1}{\mu_0}\int M\, dH$$

$$= \frac{1}{\mu_0}\int\left[\left(\frac{1}{N_o A_m}\right)\int\left(\frac{\Delta V}{a}\right)_{pick\text{-}up} dt\right] d\left(\frac{V_m}{c}\right)$$

$$= \frac{1}{(\mu_0 N_o A_m c)\, a}\int\left[\int (\Delta V)_{pick\text{-}up}\, dt\right] dV_m \qquad (13)$$

The integral on the right, in [V^2s], is obtained either from an area measurement of the M–H traces drawn by "LOSS", or the area calculated by "LOSS"; Q is then given in units of energy density, [mJ/cc]. It is important to note that the reference volume for this energy density is the conductor volume, including superconductor, non–superconducting metal, and helium coolant, but not including the conduit.

Using the sub–size sample data for this experiment, we get:

Furukawa Sub–size Conductor

d_i =	8.06 mm
d_o =	9.84 mm
D_i =	101.6 mm
A_m =	1815 mm^2
N_o =	34
$(\mu_0 N_o A_m c)^{-1}$ =	24610 (mJ/cc)/(V^2s)

Hitachi Cable Sub–size Conductor

d_i =	6.0 mm
d_o =	8.4 mm
D_i =	100.0 mm
A_m =	1146 mm^2
N_o =	36
$(\mu_0 N_o A_m c)^{-1}$ =	36800 (mJ/cc)/(V^2s)

3. EXPERIMENTAL PROCEDURE

All of the data were collected by a digital memory system (DM7100) capable of storing 4000 data points per channel. Two channels were used: one for the voltage across the background magnet measurement resistor, and one for the amplified pick-up coil signal. Each test was performed using a maximum current in the background magnet of 100A, 200A, or 300A. The data from each test was subsequently transferred from the digital memory to files on magnetic computer disk. Each file contained one test run: in the case of hysteresis measurements, one ramp up and ramp down between zero and maximum magnet current; in the case of coupling losses, one exponential "dump" from a maximum magnet current.

3.1 Hysteresis Loss Measurement

Hysteresis loss measurements were made by ramping the background field magnet's current at a set rate, stopping five or six times during ramp-up and ramp-down (see fig. 5). This "stopping" produced a "stair-like" current form in the background field magnet, and the current was stopped long enough for the coupling currents in the sample to decay away. This procedure was performed for each sample, ramping the current in the background magnet to 100A or to 300A.

In addition, the background magnet was ramped to a maximum of 100A, 200A, or 300A without the "stair-like" wave form, as in fig. 6; the magnetization produced in these cases would include coupling losses as well as hysteresis loss.

3.2 Coupling Loss Measurement

Coupling loss data were acquired by first, setting the background magnet at a constant current of 100A, 200A, or 300A long enough for any resistive currents in the sample to decay away, and then discharging the background magnet through a resistor. The discharge produced an exponential decay in the magnetic field (see fig. 7). The "dump" resistors (with the associated natural decay constants) used here were: 0.05 Ω (2200 ms), 0.1 Ω (1100 ms), 0.25 Ω (440 ms), 0.5 Ω (220 ms), 0.75 Ω (146.7 ms), 1.0 Ω (110 ms), 1.5 Ω (73.3 ms), and 2.0 Ω (55 ms). The M-H plot of this exponential "dump", then, included both the hysteresis and coupling losses experienced during the decay.

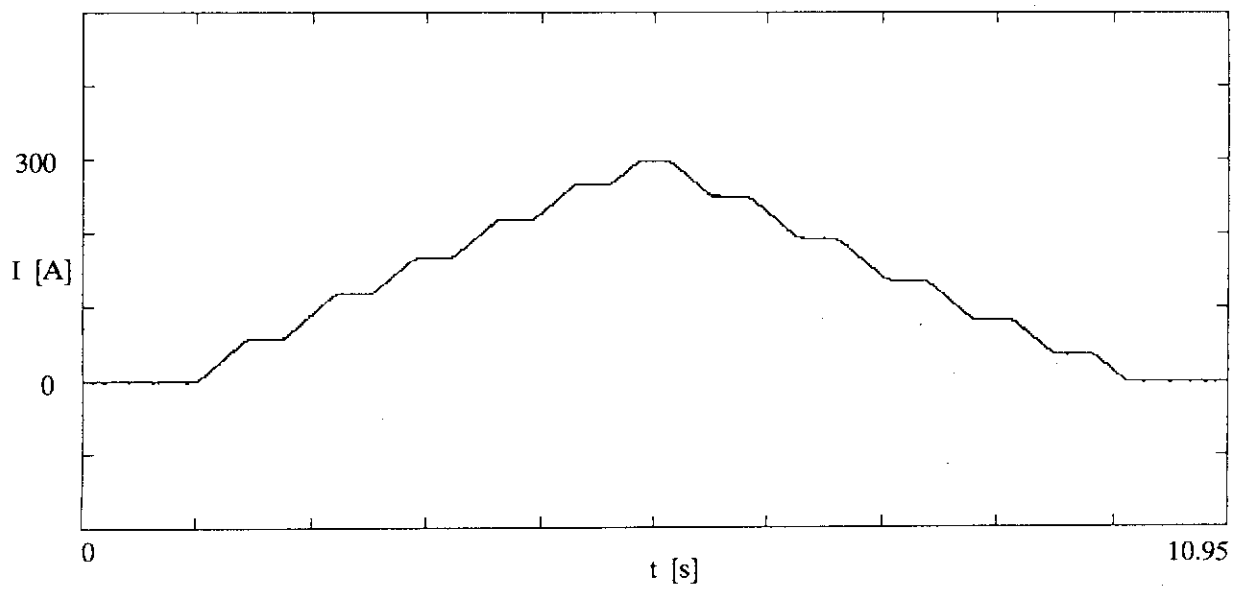

Fig. 5 A typical "stair-like" current trace in the background field magnet used to help determine the hysteresis loss in the sample. On the "plateaus" where the current did not change, any coupling currents in the sample would decay away, leaving only the hysteresis part.

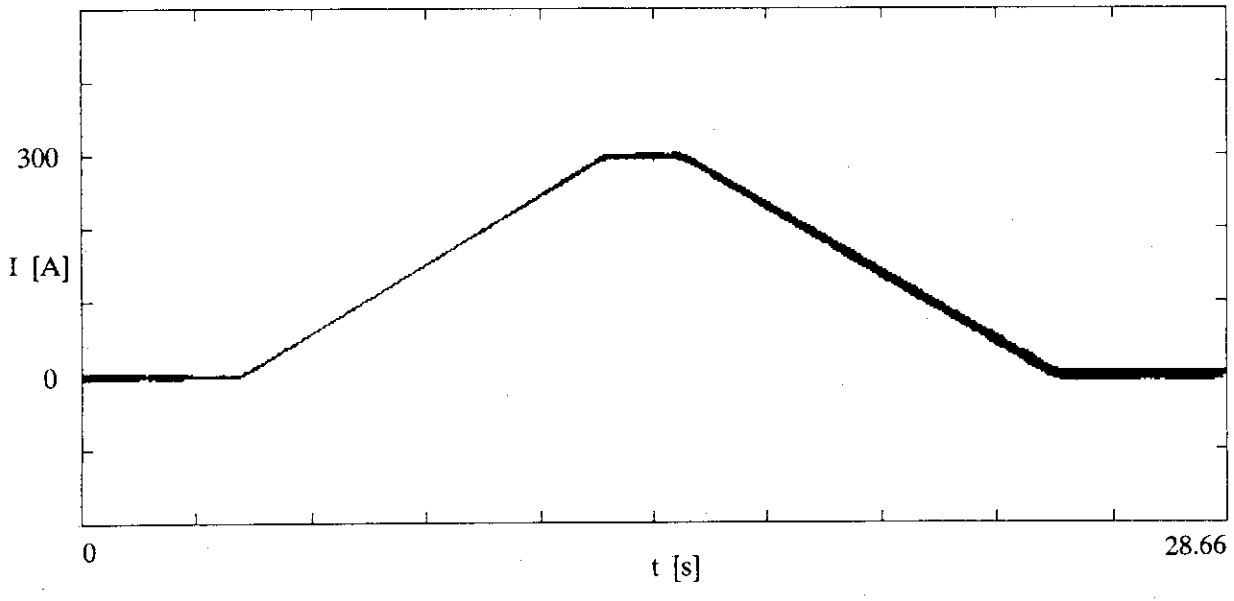

Fig. 6 A typical ramp-up and down of the current in the background field magnet. The signal from the pick-up coils associated with such a trace includes both hysteresis loss and also some coupling current loss, which depends on the ramping speed.

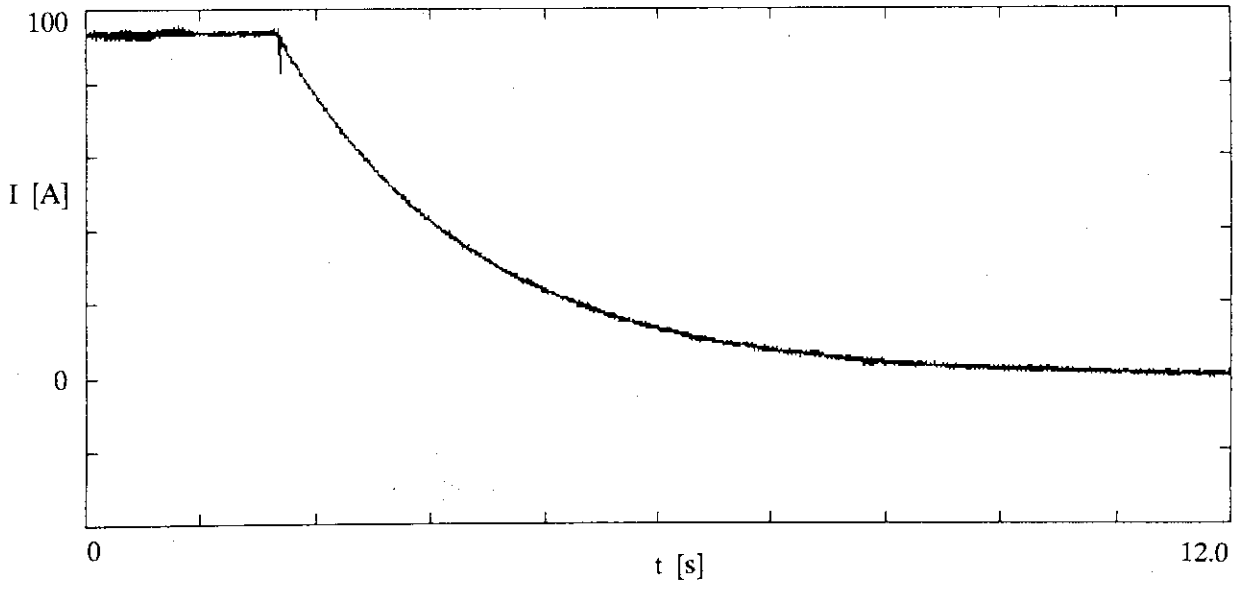

Fig. 7 A typical "dump" of the background field, made by allowing the current in the background field magnet to decay exponentially through a resistor. The signal from the pick-up coils associated with these traces was used to estimate the coupling loss and coupling time constant.

4. ANALYSIS

Most of the raw data for the loss calculations were taken directly from the printed graphs of the magnetization (time integral of the pick-up coil signal) versus the background field (voltage drop across the background magnet measurement resistor). These graphs were generated by the program "LOSS".

Because the I_{max} values taken from the current supply during the test runs slightly disagreed with the data used on the M-H curves, an uncertainty of about 3% exists in the values of maximum field.

4.1 Hysteresis Loss

Since the rather sensitive pick-up coils tended to drift slightly from a zero reading at zero field during a test run, it was necessary to change the magnetization offset in the program "LOSS". This alteration forced the magnetization curve to begin and end at the same point; in this analysis, the beginning point was placed at the origin for convenience. The program then used a linear difference between the drift and the imposed offset to calculate and plot the magnetization curve.

For tests where the maximum background magnet current was 100A or 300A, the current was ramped in a "stair-like" manner. During those periods when the current was not changing, the coupling currents decayed away leaving only the hysteresis--or "time-independent"-- magnetization of the sample. The trace on the M-H graph during this stair-like ramping, therefore, indicates points on the hysteresis curve (see figs. 8-11). With a knowledge of the general form of the hysteresis loop, an approximate curve was drawn through the hysteresis points on the graph; the area was then measured using a roller planimeter, and subsequently converted to energy loss through the appropriate conversion factor. In addition, for the data from the Furukawa sample, a polynomial curve-fit to the data was found; comparison with the area measurement showed good agreement. No curve fit for the Hitachi data was attempted.

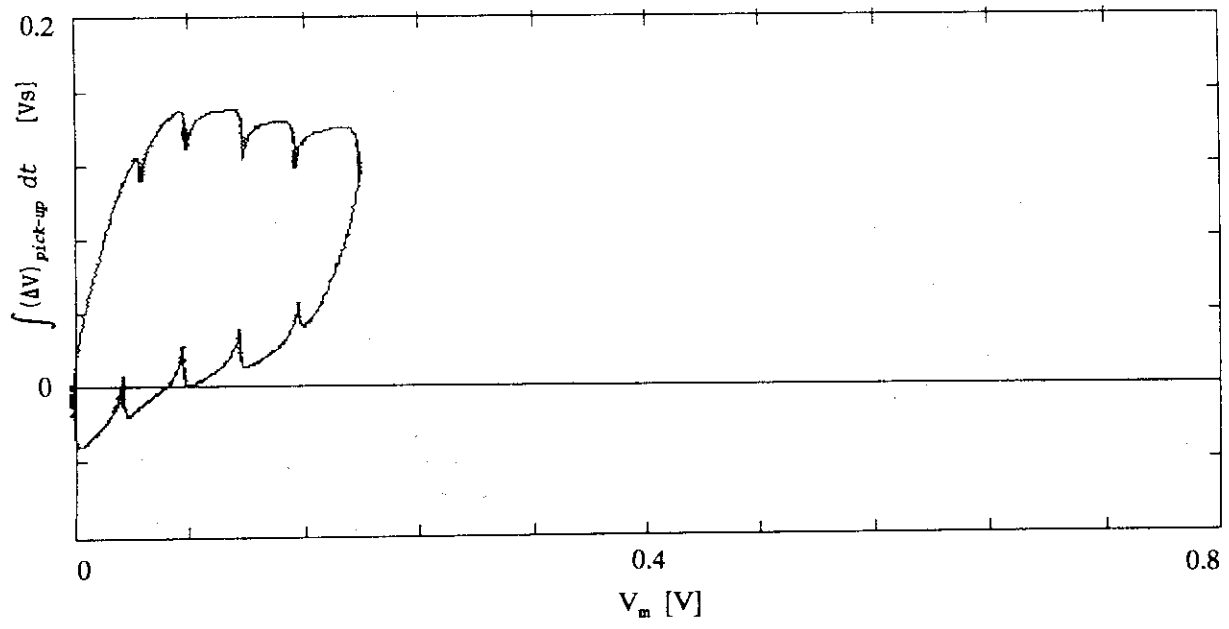

Fig. 8 The M-H trace computed by the computer program "LOSS" during a current form in the background field magnet like the one in fig. 5. In this case, I_{max}=100 A, and the trace is for the Furukawa sample. The hysteresis curve, which passes through the "spiked" points, can be drawn, and the area measured to determine the hysteresis loss.

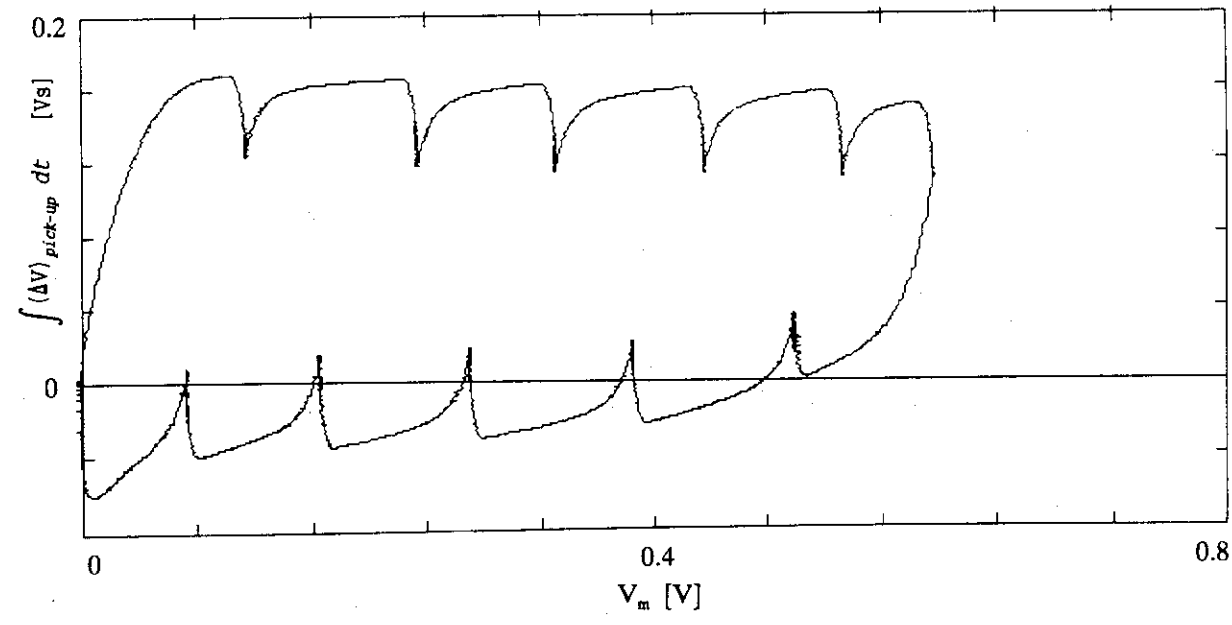

Fig. 9 The M-H trace for the Furukawa sample like the one in fig. 8, except here I_{max}=300 A. The coordinates of the "spiked" points from figs. 7 and 8 were used in a polynomial curve fit (see figs. 12 and 13).

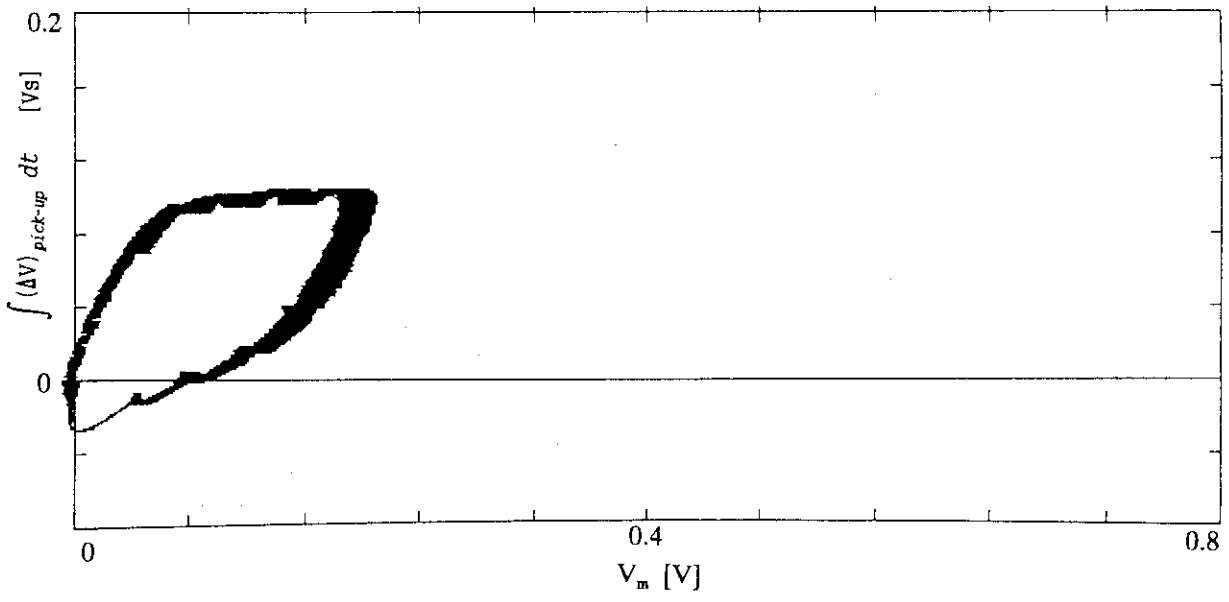

Fig. 10 The M-H trace for the Hitachi sample like the one in fig. 8.

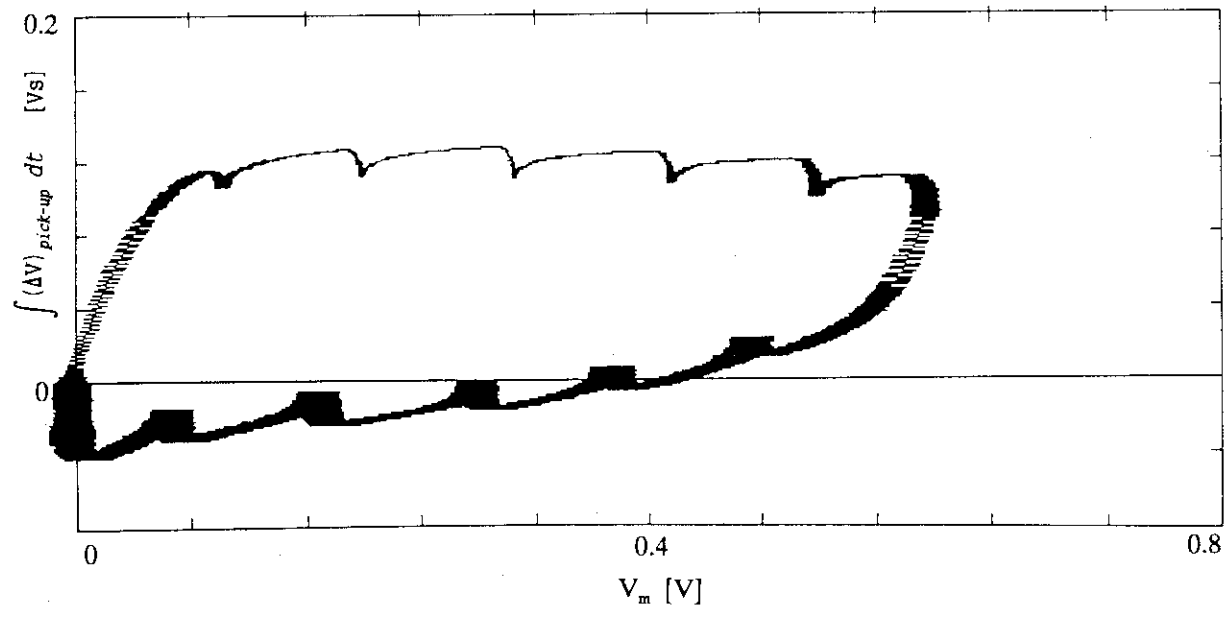

Fig. 11 The M-H trace for the Hitachi sample like the one in fig. 8, except here I_{max}=300 A. Unlike the Furukawa sample, no polynomial curve fit was attempted with this data.

The results are as follows:

Area Measurement

Furukawa Sample

Reference	I_{max}	Area enclosed	Q_{hys}
Fig. 8	100 A	0.01525 V^2/s	3.75 mJ/cc
Fig. 9	300 A	0.05064 V^2/s	12.46 mJ/cc

Hitachi Cable Sample

Reference	I_{max}	Area enclosed	Q_{hys}
Fig. 10	100 A	0.01150 V^2/s	4.23 mJ/cc
Fig. 11	300 A	0.05398 V^2/s	19.86 mJ/cc

Polynomial Curve-fit

Furukawa Sample

The curve from V_m=0 V up to V_m=V_{max} (V_m in volts) was approximated by using the hysteresis curve data points (see appendix for data points used). A cubic function was found through the first five data points, and another cubic was found through the last seven:

$$M_1[V\cdot s] = 4.092\,V_m - 41.78\,V_m^2 + 134.9\,V_m^3 \quad ,0 \le V_m \le 0.123V \tag{14}$$

$$M_2[V\cdot s] = 0.1318 - 0.09693\,V_m + 0.1516\,V_m^2 - 0.08590\,V_m^3 \quad , \quad V_m \ge 0.123V \tag{15}$$

The curve from V_m=V_{max} down to V_m=0 depends on V_m; for I_{max}=100 A, the curve is:

$$M_3[V\cdot s] = 0.6622\,V_m - 7.800\,V_m^2 + 37.49\,V_m^3 \quad ,0 \le V_m \le 0.1965V \tag{16}$$

(see fig. 12). For I_{max}=300 A a cubic curve did not fit the data well, so a 5th-order polynomial was used:

$$M_4[V\cdot s] = 0.1536\,V_m - 0.8445\,V_m^2 + 4.733\,V_m^3 - 13.51\,V_m^4 + 13.61\,V_m^5 \quad ,0 \le V_m \le 0.5946V \tag{17}$$

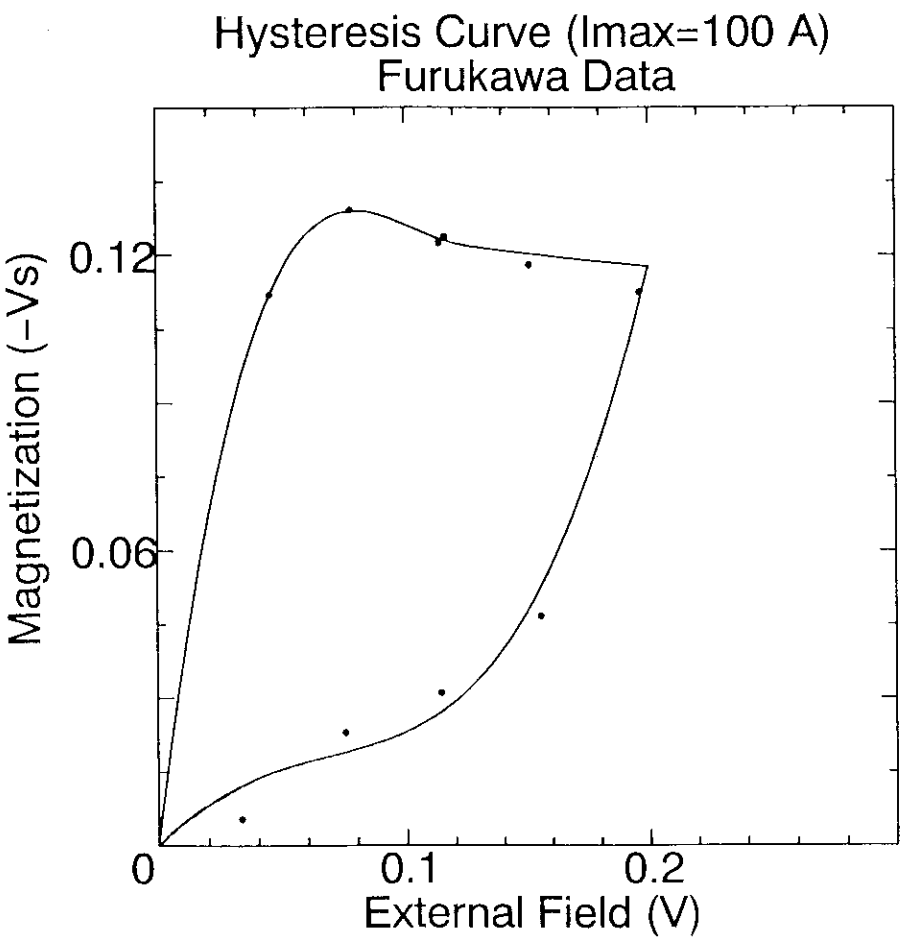

Fig. 12 The curve-fit trace for the Furukawa sample when I_{max}=100 A. The top part of the curve was computed using data from both figs. 8 and 9, since the hysteresis curve is the same ; the bottom of the curve uses the data from fig. 8 only.

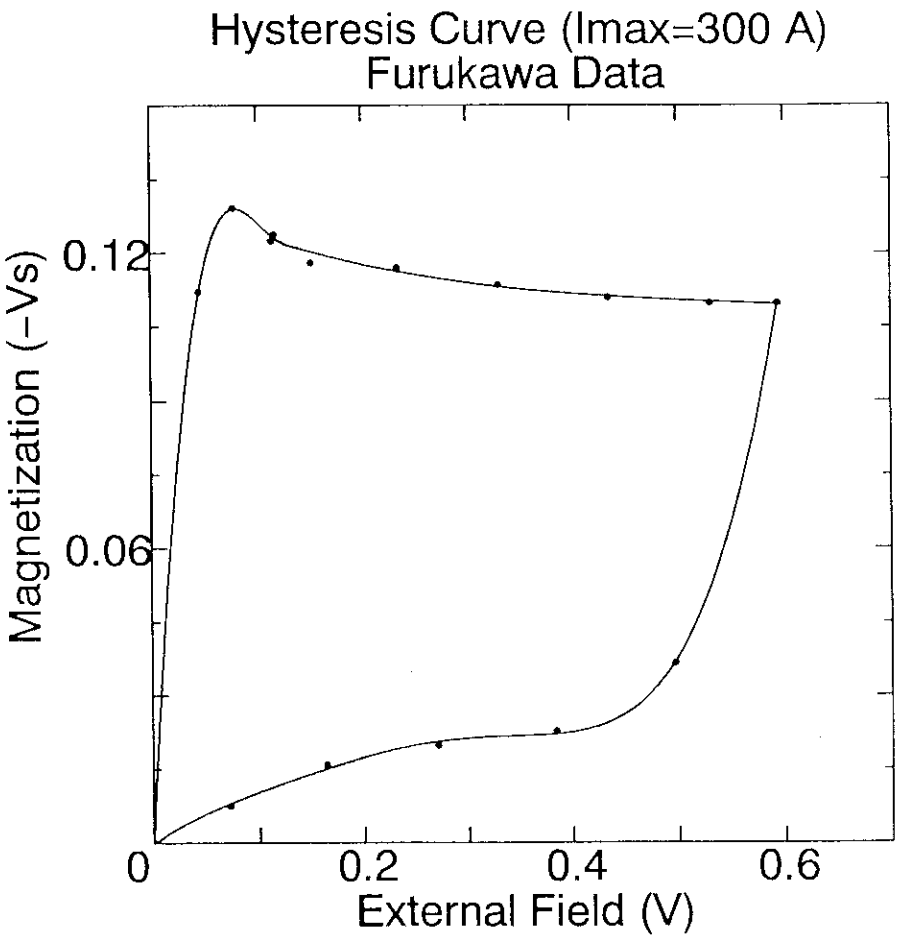

Fig. 13 The curve-fit trace for the Furukawa sample when I_{max}=300 A. The top part of the curve was computed using data from both figs. 8 and 9, while the bottom of the curve used the data from fig. 9 only.

(see fig. 13). With these curve-fits, the hysteresis loss is easily calculated:

$$A_{hys,100A} = \int_0^{0.123} M_1\, dV_m + \int_{0.123}^{0.1965} M_2\, dV_m - \int_0^{0.1965} M_3\, dV_m$$
$$= 0.01454\ V^2 \cdot s$$

or Q_{hys}=3.58 mJ/cc for I_{max}=100 A; and

$$A_{hys,300A} = \int_0^{0.123} M_1\, dV_m + \int_{0.123}^{0.5946} M_2\, dV_m - \int_0^{0.5946} M_4\, dV_m$$
$$= 0.05112\ V^2 \cdot s$$

or Q_{hys}=12.58 mJ/cc for I_{max}=300 A. Note that the hysteresis loss predicted by the curve fits is close to that of the area method.

Hitachi Cable Sample

No curve-fit was calculated.

For a maximum magnet current of 200 A, no "stair-like" ramping was done, so the hysteresis loss had to be calculated in some other way. The curve shape for the ramp-up part was the same as for the 300 A case, but the shape during ramp-down would have been speculation. Initially, an effort was made to determine the coupling time constant first (from the exponential dump data), and then use this to calculate the hysteresis loss during a dump. With a knowledge of the top part of the hysteresis curve, the net hysteresis loss could be calculated. From the theory, if the maximum field were the same for two exponential dumps through different dump resistors, the coupling time constant should be:

$$\tau_{cpl} = C - \sqrt{C^2 - \tau_1 \tau_2} \tag{18}$$

where

$$C = \frac{B_{max}^2}{4\mu_0 (Q_{int,1} - Q_{int,2})} (\tau_1 - \tau_2) - \frac{1}{2}(\tau_1 + \tau_2) \tag{19}$$

(The Q_{int} here can be determined by multiplying the value of M_{int} by the appropriate conversion factor.) This coupling time constant could then be used in eq. 7 to determine the coupling loss, and, with some simple arithmetic, the hysteresis loss could be calculated. Unfortunately, this calculation yielded a large range of possible hysteresis loss values, depending on which pair of trials were selected for the computation. This wide range is due in part to error propagation through the numerous calculations, and in part to insisting that the coupling time constant be truly constant, as the theory indicates.

Instead, an approximation was used. During a linear rise and fall ramping of the background field, if the rise time T is very long compared to the coupling time constant, then [see Tsuji et al.]:

$$\begin{aligned} Q_{cpl} &\sim B_{max}^2 \frac{\tau_{cpl}}{T} \\ &\sim I_{max} \dot{I} \tau_{cpl} \end{aligned} \tag{20}$$

For two tests having the same ramping speed and coupling time constant (as in figs. 14 and 15), we can compute:

$$Q_{hys,2} = Q_{int,2} - (Q_{int,1} - Q_{hys,1})\left(\frac{I_{max,2}}{I_{max,1}}\right) \tag{21}$$

where Q_{int} is found by multiplying the correct conversion factor times the M_{int} value computed by "LOSS". Using the values for hysteresis loss when I_{max}=100 A calculated above, we can find the hysteresis loss for when I_{max}=200 A:

Furukawa Sample

Reference	dI/dt	I_{max}	M_{int}	Q_{hys}
Fig. 14	750 A/min	100 A	0.02269 V^2s	3.58 mJ/cc
Fig. 14	750 A/min	200 A	0.04499 V^2s	7.08 mJ/cc

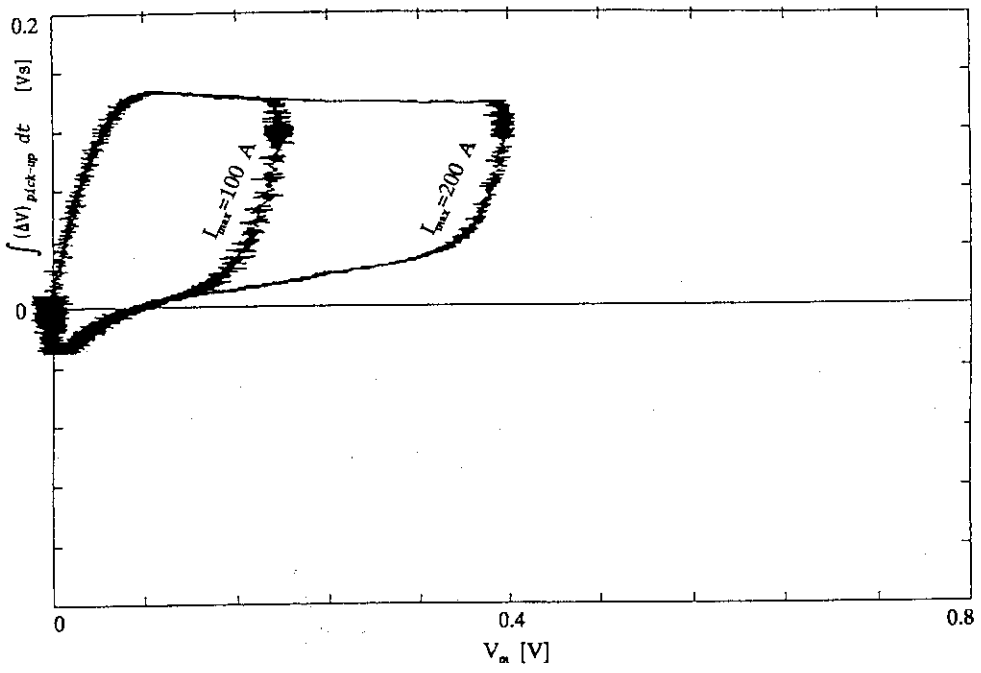

Fig. 14 The M-H traces for the Furukawa sample with I_{max}=100 A and I_{max}=200 A using a current form in the background field magnet like the one in fig. 6. The ramping speed was 750 A/min, and the amplifier was set at 100. "LOSS" computed the areas on the M-H curve as M_{int}=0.02269 V^2s and M_{mint}=0.0449853 V^2s for I_{max}=100 A and I_{max}=200 A, respectively.

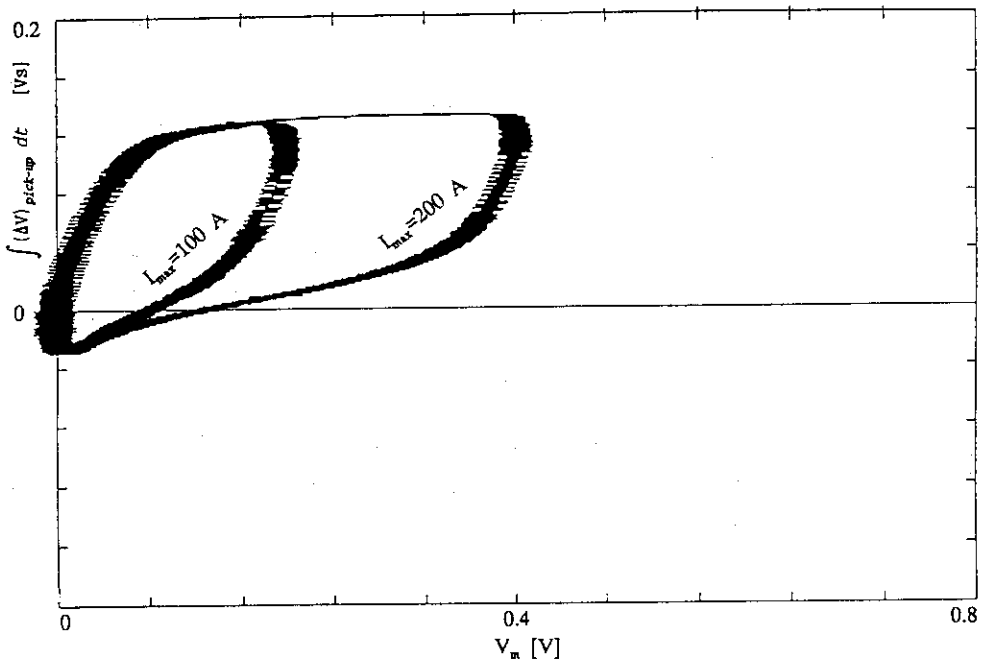

Fig. 15 The M-H traces for the Hitachi sample with I_{max}=100 A and I_{max}=200 A using a current form in the background field magnet like the one in fig. 6. The ramping speed was 2000 A/min, and the amplifier was set at 100. "LOSS" computed the areas on the M-H curve as M_{int}=0.01723 V^2s and M_{mint}=0.0407309 V^2s for I_{max}=100 A and I_{max}=200 A, respectively.

Hitachi Cable Sample

Reference	dI/dt	I_{max}	M_{int}	Q_{hys}
Fig. 15	2000 A/min	100 A	0.01723 V^2s	4.23 mJ/cc
Fig. 15	2000 A/min	200 A	0.04073 V^2s	10.0 mJ/cc

We have arbitrarily chosen to use the hysteresis loss predicted by the curve-fit in computing the loss for the Furukawa sample.

4.2 Coupling Loss

The coupling loss was determined from the trace of M vs. H during an exponential "dump" of the external magnetic field. During the experiment, at the instant the dump actually began, the magnet current dipped momentarily to extremely low values. This behavior seemed to become more pronounced as the dump resistor was increased. The pick-up coil signal seemed to be affected very little, but the undesirable behavior of the magnet (perhaps as a result of interaction with the power supply) caused large errors in the numerical calculations later. Because much of the loss characteristics occurred during the very time the background magnet signal dropped, the data during the first few milliseconds after dump initialization was modified to approximate a normal exponential decay on some of the files.

Since the rather sensitive pick-up coils tended to drift slightly from a zero reading at zero field during a test run, it was necessary to change the magnetization offset in the program "LOSS". This alteration forced the magnetization plot to begin at the top of the magnetization curve (for the I_{max} used during the test run) and end at the bottom of the magnetization curve (where I=0). In this analysis, the beginning of the test run was set at zero magnetization and the end at the negative value of the magnetization at I_{max} for convenience. The program then used a linear difference between the drift and the imposed offset to calculate and plot the "dump" curve as well as M_{int} (the area under the curve). Figs. 16 and 17 show the M-H plots for some selected external field natural decay time constants.

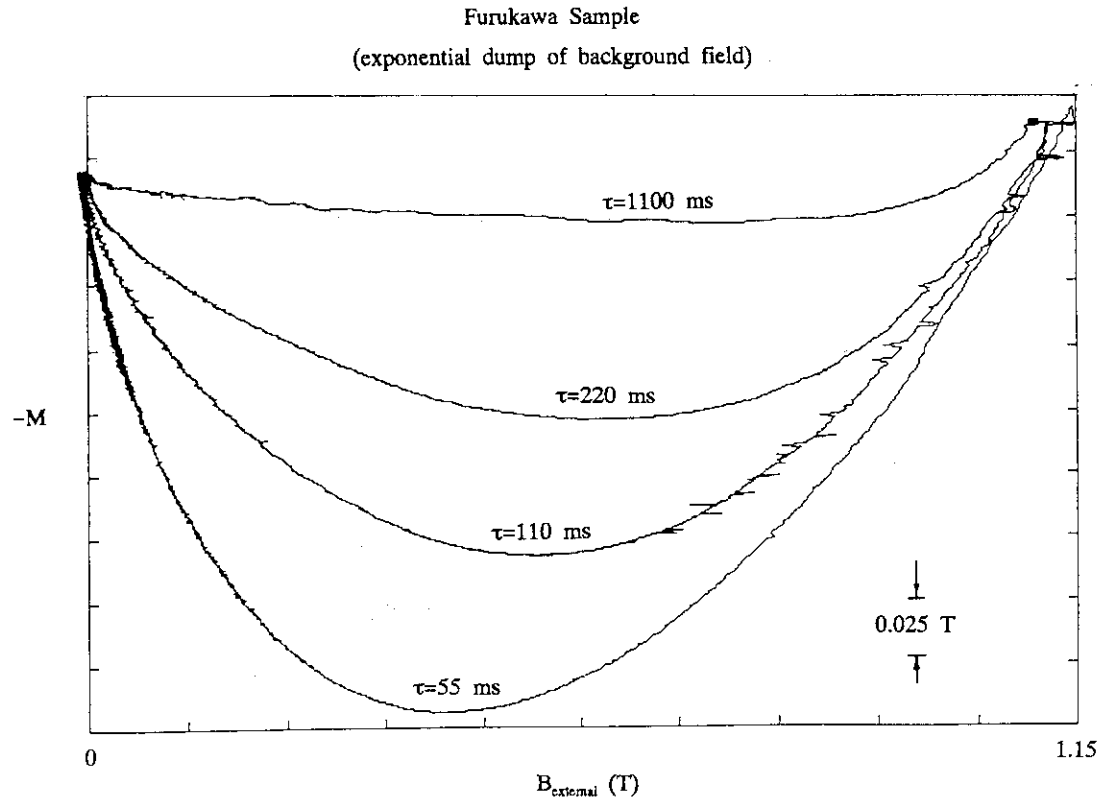

Fig. 16 Some M-H traces for the Furukawa sample during an exponential dump of the background field magnet (like the one in fig. 7), from I_{max}=300 A, for some different natural decay constants. Note the scale, in tesla, on both axes.

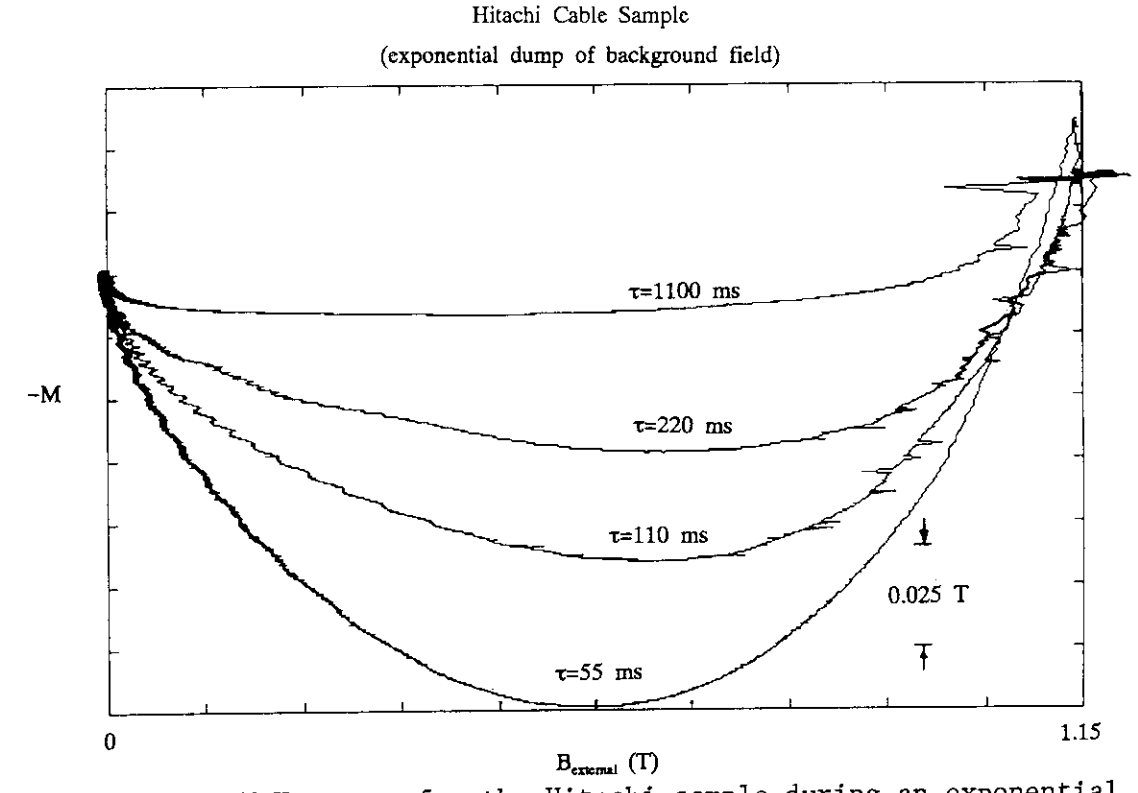

Fig. 17 Some M-H traces for the Hitachi sample during an exponential dump of the background field magnet (like the one in fig. 7), from I_{max}=300 A, for some different natural decay constants. Note the scale, in tesla, on both axes.

The top of the magnetization curve was taken from the hysteresis plot:

Furukawa Sample (a=100)

I_{max}	M_{top} [Vs]	V_{max}
100 A	0.1126 Vs	0.1965 V
200 A	0.1110 Vs	0.3947 V
300 A	0.1099 Vs	0.5946 V

Hitachi Cable Sample (a=100)

I_{max}	M_{top} [Vs]	V_{max}
100 A	0.0923 Vs	0.1958 V
200 A	0.0922 Vs	0.3937 V
300 A	0.0903 Vs	0.5903 V

The value M_{int} calculated by "LOSS" contains the coupling loss (A_{cpl}) plus a portion of the hysteresis loss and other non-significant area (called A_{hys+} herein)--see fig. 18. This A_{hys+} must be calculated and subtracted from M_{int} in order to determine the coupling loss. There are two simple methods for calculating A_{hys+} in this case: measure the area on a hysteresis graph (if the whole hysteresis curve is known), or use $A_{hys+}=A_{hys}-A_{xtr}+A_{non}$ (see fig. 18 for the meaning of these areas). For our case, the first method is not possible for I_{max}=200 A.

The first method is perhaps better for I_{max}=100 A or 300 A because it involves fewer area measurements. Using a roller planimeter, we get:

Furukawa Sample

Reference	I_{max}	A_{hys+}
Fig. 8	100 A	0.0151 V^2s
Fig. 9	300 A	0.0501 V^2s

Hitachi Cable Sample

Reference	I_{max}	A_{hys+}
Fig. 10	100 A	0.0143 V^2s
Fig. 11	300 A	0.0475 V^2s

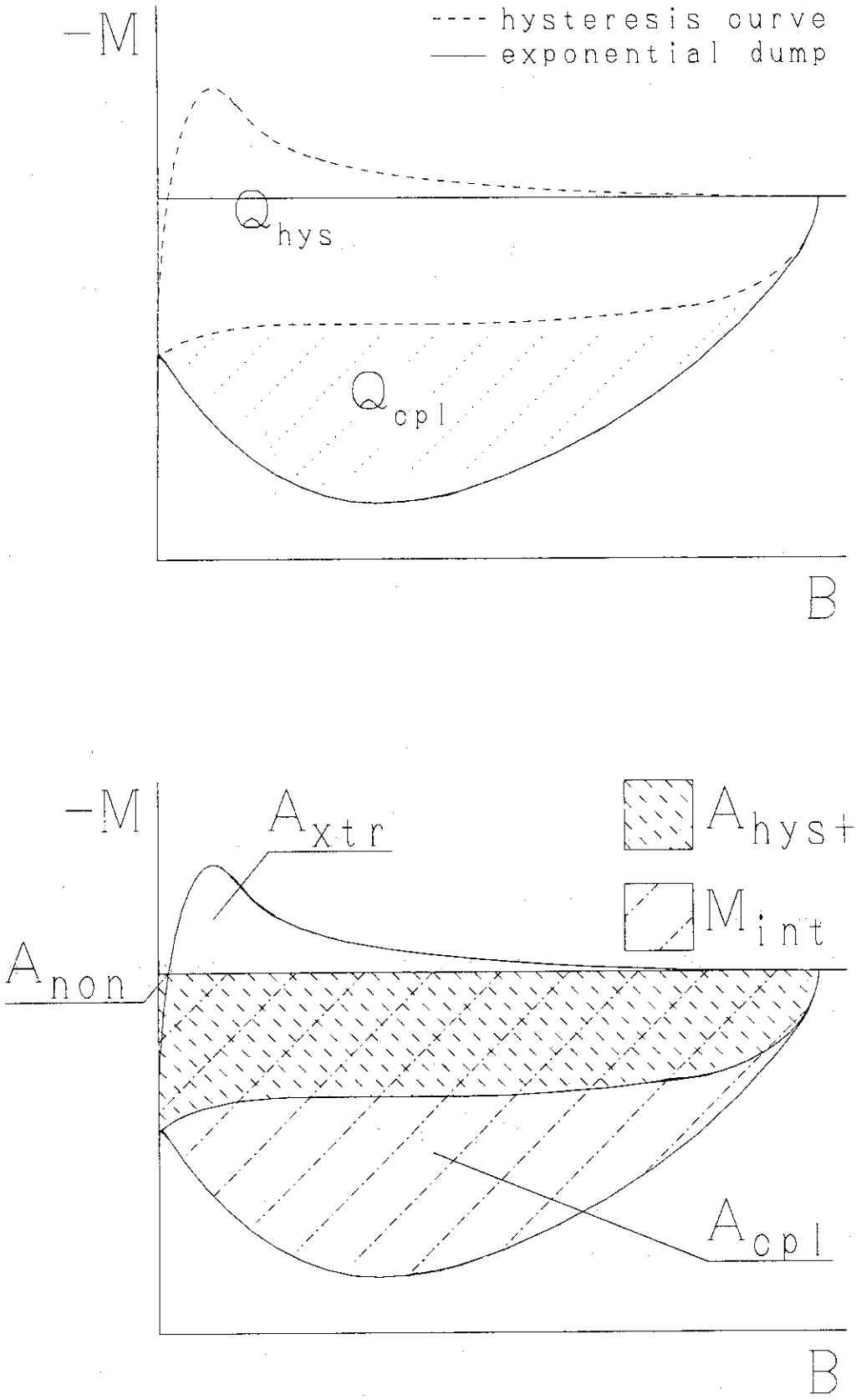

Fig. 18 Graphs showing the significance of areas on the M-H curve, and defining some areas used to estimate the coupling loss.

For I_{max}=200 A, we measure the A_{xtr} and A_{non} areas and use Q_{hys} from above with the correct conversion factor to obtain:

Furukawa Sample (a=100)

A_{hys}	A_{xtr}	A_{non}	A_{hys+}
2.885×10^{-2} V^2s	3.335×10^{-3} V^2s	8.513×10^{-4} V^2s	0.0313 V^2s

Hitachi Cable Sample (a=100)

A_{hys}	A_{xtr}	A_{non}	A_{hys+}
2.717×10^{-2} V^2s	2.658×10^{-3} V^2s	3.156×10^{-3} V^2s	0.0268 V^2s

Of course, the A_{hys+} calculation for the Furukawa sample can also be carried out using the polynomial curve-fit to estimate A_{xtr} and A_{non}; the results will be similar.

The coupling loss depended on the decay constant of the external magnetic field, according to:

$$\tau = \frac{L}{R_{dump}} \tag{22}$$

where L=background field magnet inductance=0.11 H.

4.3 Coupling Time Constant

Knowing the coupling loss allows a calculation of the coupling time constant from the theory:

$$\tau_{cpl} = \frac{\tau}{\left(\frac{B_{max}^2}{2\mu_0 Q_{cpl}}\right) - 1} \tag{23a}$$

or, specifically for this experiment:

$$\tau_{cpl} = \frac{\tau}{\left(5.794\times10^{-3}\frac{mJ/cc}{A^2}\right)\frac{I_{max}^2}{Q_{cpl}} - 1} \tag{23b}$$

This coupling time constant was calculated for each test, but the values showed a large range: another form of data analysis was required.

Rearranging the theoretical formula for coupling loss, we can write:

$$\tau = \left(\frac{B_{max}^2 \tau_{cpl}}{2\mu_0}\right)\left(\frac{1}{Q_{cpl}}\right) - \tau_{cpl} \tag{24}$$

So, for constant B_{max} (i.e. constant I_{max}), a graph of τ versus $(1/Q_{cpl})$ should be a straight line with the coupling time constant as the intercept. Unfortunately the data did not lend itself well to a straight line curve-fit, because the smaller coupling loss values were weighted far more heavily than the other data points: a small error in their values corresponded to large errors in the coupling time constant value.

Finally, a "best-guess" curve considering all of the data was adopted: the curve

$$Q_{cpl} = \left(5.794 \times 10^{-3} \frac{mJ/cc}{A^2}\right) I_{max}^2 \left(\frac{\tau_{cpl}}{\tau + \tau_{cpl}}\right) \tag{25}$$

was plotted with different values of τ_{cpl} until the best value was estimated.

5. RESULTS

5.1 Hysteresis Loss Results

The hysteresis losses for the sample, as a function of external field, are summarized by:

	HYSTERESIS LOSS	
Maximum Field	Furukawa Sample	Hitachi Cable Sample
1.15 T	12.6 mJ/cc	19.9 mJ/cc
0.76 T	7.1 mJ/cc	10.0 mJ/cc
0.38 T	3.6 mJ/cc	4.2 mJ/cc

Figures 19 and 20 show the hysteresis curves for the B_{max}=1.15 T case.

The above results agree well with the hysteresis loss measurements performed on the strands of the conductors. For example, at 1.15 T, the Furukawa conductor measured a loss of 50.0 mJ per cubic centimeter of non-copper metal, while the individual strand measurement recorded a value of 51.6 mJ per cubic centimeter of non-copper metal; and the Hitachi Cable conductor measured a hysteresis loss of 77.9 mJ per cubic centimeter of non-copper metal, while the individual strand measurement recorded a value of 70.6 mJ per cubic centimeter of non-copper metal. (The results of A.C. loss measurements performed on the individual strands are to be published in a subsequent report.) In both cases, the values are within about 10% of each other.

5.2 Coupling Time Constant Results

Using a curve-fit based on the theory (figs. 21 and 22), the coupling time constant is approximately:

COUPLING LOSS TIME CONSTANT	
Furukawa Sample	Hitachi Cable Sample
27 (±5) ms	11 (±5) ms

The theory does not seem to completely explain the loss behavior at smaller time constants. More investigation into this matter, accompanied by more data (specifically with smaller decay constants, meaning larger dump resistors), would be advantageous.

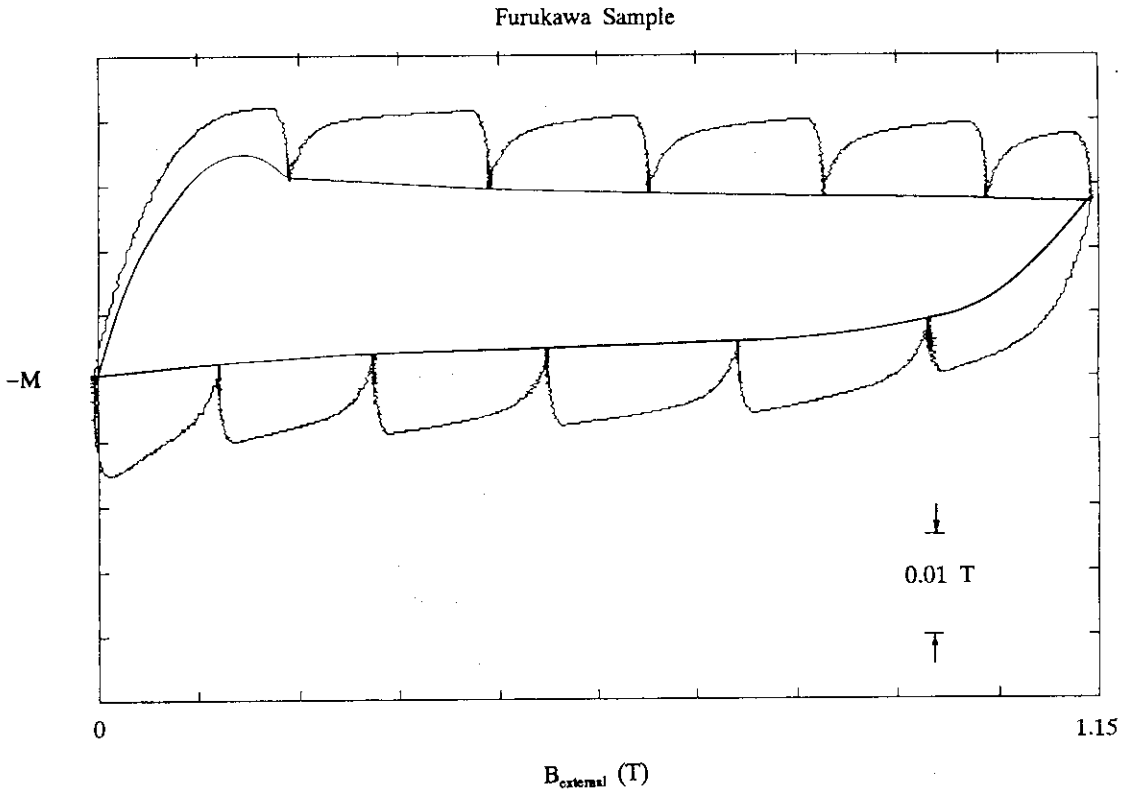

Fig. 19 Hysteresis curve for the Furukawa sample when I_{max}=300 A. Note the scale, in tesla, on both axes.

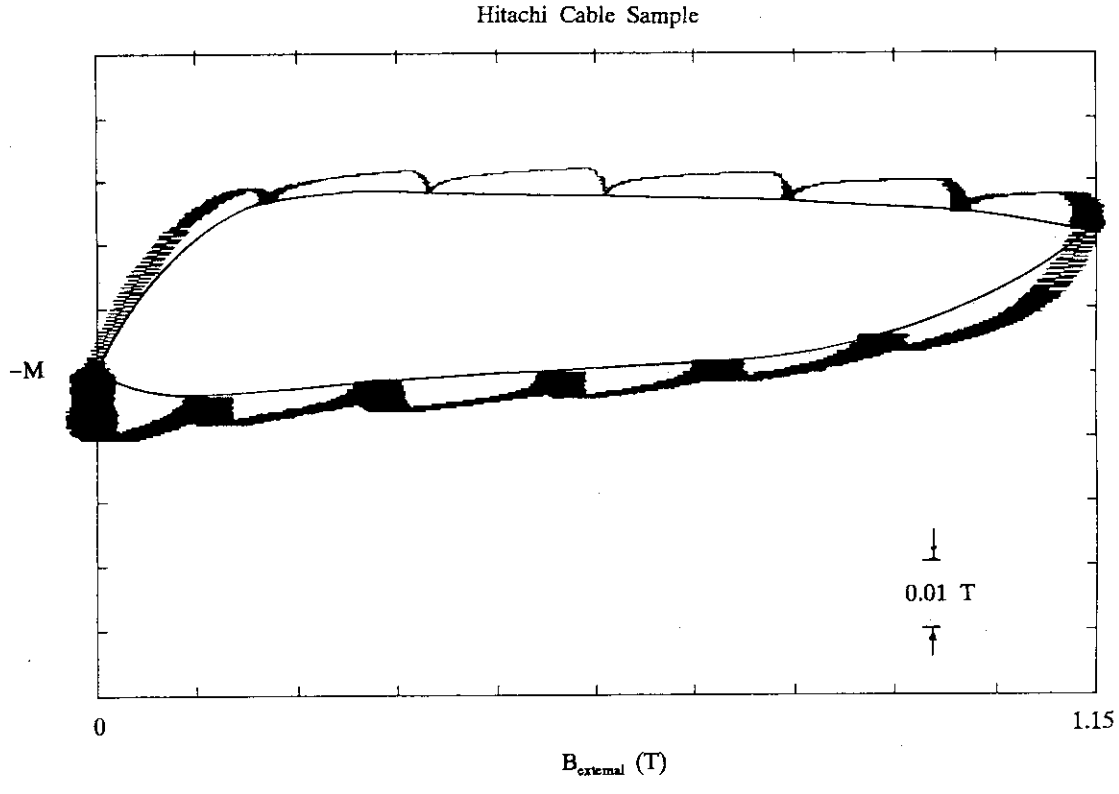

Fig. 20 Hysteresis curve for the Hitachi sample when I_{max}=300 A. Note the scale, in tesla, on both axes.

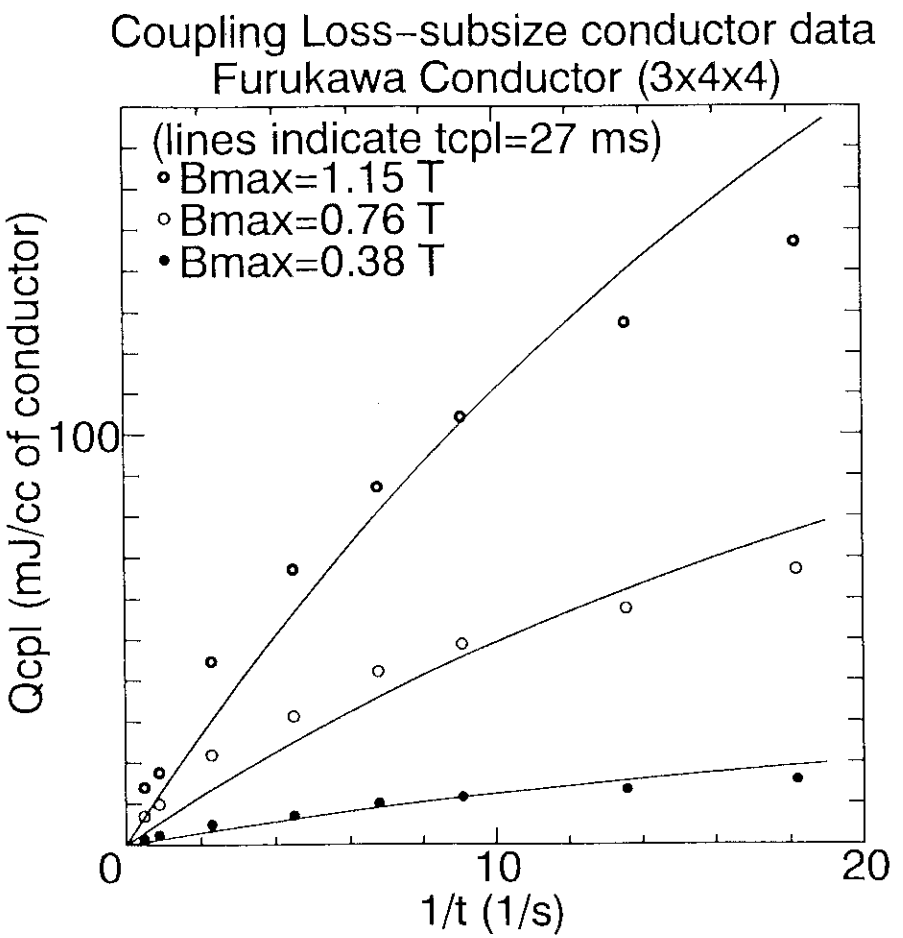

Fig. 21 Graph of the coupling loss during an exponential dump of the background field versus the inverse of the natural decay time constant of the background field for the Furukawa sample. The lines indicate the theoretical prediction based on a "best guess" value of 27 ms for the coupling time constant.

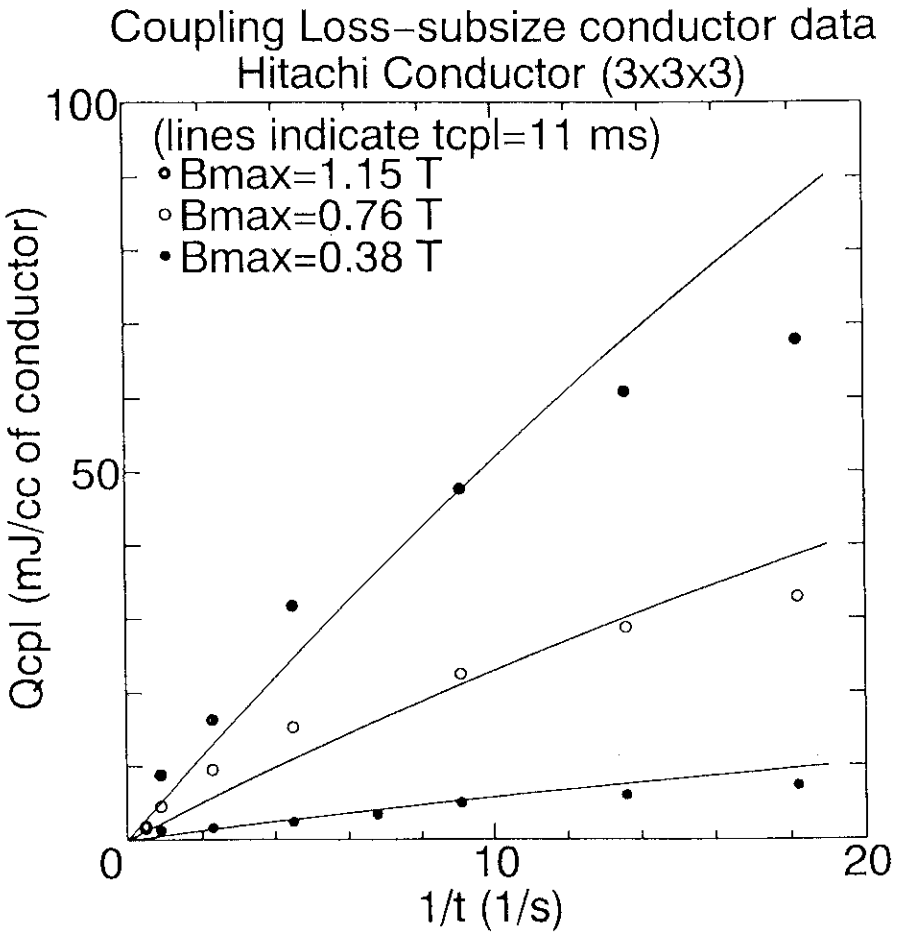

Fig. 22 Graph of the coupling loss during an exponential dump of the background field versus the inverse of the natural decay time constant of the background field for the Hitachi sample. The lines indicate the theoretical prediction based on a "best guess" value of 11 ms for the coupling time constant.

Although the Hitachi Cable sample showed a smaller coupling time constant, the effects of cabling twist pitch, number of strands, and void fraction have not been considered. Based on the cabling twist pitch alone, we would expect the Hitachi Cable sample to have a coupling time constant of about 16 ms if it were cabled like the Furukawa sample.

6. CONCLUSION

The hysteresis loss measurements of the sub-size conductors agreed well with the results of similar measurements made on the individual strands. (Results on the A.C. loss measurments for the individual strands is to be published in another report.) The magnitude of the losses for the particular conductors tested here compares quite favorably with the hysteresis losses of conductors manufactured in the past, indicating definite progress toward realizing a reliable pulse coil for the ITER. However, the coupling time constant for both sub-size samples is rather large--about 10 times larger than the theoretical predictions for a single strand.

It would be advantageous to know what effect different void fractions, different chromium thicknesses (as the strand coating material), and different cabling twist pitches have on the coupling time constant of the coupling currents between the strands, although such knowledge naturally comes as a result of increased study and expense. However, reducing the coupling loss is of paramount importance in the design and manufacture of polodial coils for large tokamak machines like the ITER, and, indeed, for all superconducting magnets in general.

REFERENCES

1. L. Bottura, et al., *ITER Magnets*, ITER Documentation Series, No. 26, IAEA, Vienna, 1991.

2. H. Tsuji, et al., "Pulsed Field Loss Characteristics of the Japanese Test Coil for the Large Coil Task", *IEEE Transactions on Magnetics*, MAG-17, 1981, pp. 42-45.

3. M. Wilson, *Superconducting Magnets*, Clarendon Press, Oxford, 1983.

Although the Hitachi Cable sample showed a smaller coupling time constant, the effects of cabling twist pitch, number of strands, and void fraction have not been considered. Based on the cabling twist pitch alone, we would expect the Hitachi Cable sample to have a coupling time constant of about 16 ms if it were cabled like the Furukawa sample.

6. CONCLUSION

The hysteresis loss measurements of the sub-size conductors agreed well with the results of similar measurements made on the individual strands. (Results on the A.C. loss measurments for the individual strands is to be published in another report.) The magnitude of the losses for the particular conductors tested here compares quite favorably with the hysteresis losses of conductors manufactured in the past, indicating definite progress toward realizing a reliable pulse coil for the ITER. However, the coupling time constant for both sub-size samples is rather large--about 10 times larger than the theoretical predictions for a single strand.

It would be advantageous to know what effect different void fractions, different chromium thicknesses (as the strand coating material), and different cabling twist pitches have on the coupling time constant of the coupling currents between the strands, although such knowledge naturally comes as a result of increased study and expense. However, reducing the coupling loss is of paramount importance in the design and manufacture of polodial coils for large tokamak machines like the ITER, and, indeed, for all superconducting magnets in general.

REFERENCES

1. L. Bottura, et al., *ITER Magnets*, ITER Documentation Series, No. 26, IAEA, Vienna, 1991.

2. H. Tsuji, et al., "Pulsed Field Loss Characteristics of the Japanese Test Coil for the Large Coil Task", *IEEE Transactions on Magnetics*, MAG-17, 1981, pp. 42-45.

3. M. Wilson, *Superconducting Magnets*, Clarendon Press, Oxford, 1983.

Although the Hitachi Cable sample showed a smaller coupling time constant, the effects of cabling twist pitch, number of strands, and void fraction have not been considered. Based on the cabling twist pitch alone, we would expect the Hitachi Cable sample to have a coupling time constant of about 16 ms if it were cabled like the Furukawa sample.

6. CONCLUSION

The hysteresis loss measurements of the sub-size conductors agreed well with the results of similar measurements made on the individual strands. (Results on the A.C. loss measurments for the individual strands is to be published in another report.) The magnitude of the losses for the particular conductors tested here compares quite favorably with the hysteresis losses of conductors manufactured in the past, indicating definite progress toward realizing a reliable pulse coil for the ITER. However, the coupling time constant for both sub-size samples is rather large--about 10 times larger than the theoretical predictions for a single strand.

It would be advantageous to know what effect different void fractions, different chromium thicknesses (as the strand coating material), and different cabling twist pitches have on the coupling time constant of the coupling currents between the strands, although such knowledge naturally comes as a result of increased study and expense. However, reducing the coupling loss is of paramount importance in the design and manufacture of polodial coils for large tokamak machines like the ITER, and, indeed, for all superconducting magnets in general.

REFERENCES

1. L. Bottura, et al., *ITER Magnets*, ITER Documentation Series, No. 26, IAEA, Vienna, 1991.

2. H. Tsuji, et al., "Pulsed Field Loss Characteristics of the Japanese Test Coil for the Large Coil Task", *IEEE Transactions on Magnetics*, MAG-17, 1981, pp. 42-45.

3. M. Wilson, *Superconducting Magnets*, Clarendon Press, Oxford, 1983.

APPENDIX

This appendix presents some of the data used in the report's analysis. The appendix contains Furukawa data in the first half and Hitachi data in the second. Each half contains the following:

1.) A spreadsheet showing the files of exponential dumps, as well as the major parameters associated with the analysis. The M_{int} value indicated on the spreadsheets are taken from the computer program "LOSS", and the A_{hys+} value comes from the calculations as indicated in section 4.2, "Coupling Loss". The "Modified Data" comment indicates that the first few background magnet current data points after quench initialization were modified as explained in section 4.2.

2.) A graph of the background magnet current and the pick-up coil signal (before integration), both as functions of time, as recorded during the quench. The upper curve shows the background magnet current, and the lower curve shows the pick-up coil signal. These were plotted for the I_{max}=300 A, R_{dump}=2 Ω case, to give an example of the typical data used by the program "LOSS".

3.) The family of dump curves for R_{dump}=2 Ω calculated by "LOSS". The file names are printed in the upper right-hand corner of each graph for reference.

4.) A composite graph for the R_{dump}=2 Ω exponential dumps for comparison.

A.C. Loss Data and Analysis (experiment date: June 16-18, 1993)
Furukawa Data

File Name	Imax (A)	Rdump (ohm)	t (ms)	Ampl. (x)	Mint (V^2•s)	Ahys+ (V^2•s)	tcpl (ms)	1/t (1/s)	Qhys (mJ/cc)	Qcpl (mJ/cc)	Remark
FD1-005A	100	0.05	2200.0	10	2.102E-03	1.510E-03	56.7	0.5	3.58	1.46	
FD1-01	100	0.10	1100.0	1	2.486E-04	1.510E-04	47.5	0.9	3.58	2.40	
FD1-025	100	0.25	440.0	1	3.570E-04	1.510E-04	42.2	2.3	3.58	5.07	
FD1-05	100	0.50	220.0	1	4.399E-04	1.510E-04	30.8	4.5	3.58	7.11	
FD1-075	100	0.75	146.7	1	5.585E-04	1.510E-04	30.7	6.8	3.58	10.03	
FD1-1	100	1.00	110.0	1	6.203E-04	1.510E-04	27.4	9.1	3.58	11.55	
FD1-15S	100	1.50	73.3	1	6.966E-04	1.510E-04	22.1	13.6	3.58	13.43	Modified Data
FD1-2	100	2.00	55.0	1	7.896E-04	1.510E-04	20.5	18.2	3.58	15.71	Modified Data

File Name	Imax (A)	Rdump (ohm)	t (ms)	Ampl. (x)	Mint (V^2•s)	Ahys+ (V^2•s)	tcpl (ms)	1/t (1/s)	Qhys (mJ/cc)	Qcpl (mJ/cc)	Remark
FD2-005A	200	0.05	2200.0	10	5.480E-03	3.133E-03	68.5	0.5	7.10	7.00	Polarity Reversal
FD2-01	200	0.10	1100.0	1	6.704E-04	3.133E-04	49.6	0.9	7.10	10.01	
FD2-025	200	0.25	440.0	1	1.159E-03	3.133E-04	46.2	2.3	7.10	22.03	
FD2-05	200	0.50	220.0	1	1.539E-03	3.133E-04	34.4	4.5	7.10	31.37	
FD2-075	200	0.75	146.7	1	1.979E-03	3.133E-04	32.6	6.8	7.10	42.21	
FD2-1	200	1.00	110.0	1	2.253E-03	3.133E-04	29.5	9.1	7.10	48.97	
FD2-15S	200	1.50	73.3	1	2.608E-03	3.133E-04	24.3	13.6	7.10	57.70	Modified Data
FD2-2	200	2.00	55.0	1	2.990E-03	3.133E-04	22.4	18.2	7.10	67.10	Modified Data

File Name	Imax (A)	Rdump (ohm)	t (ms)	Ampl. (x)	Mint (V^2•s)	Ahys+ (V^2•s)	tcpl (ms)	1/t (1/s)	Qhys (mJ/cc)	Qcpl (mJ/cc)	Remark
FD3-005A	300	0.05	2200.0	10	1.071E-02	5.011E-03	60.8	0.5	12.58	14.03	
FD3-01	300	0.10	1100.0	1	1.219E-03	5.011E-04	38.6	0.9	12.58	17.67	
FD3-025	300	0.25	440.0	1	2.322E-03	5.011E-04	41.4	2.3	12.58	44.82	
FD3-05	300	0.50	220.0	1	3.235E-03	5.011E-04	32.6	4.5	12.58	67.27	
FD3-075	300	0.75	146.7	1	4.040E-03	5.011E-04	29.4	6.8	12.58	87.10	
FD3-1	300	1.00	110.0	1	4.740E-03	5.011E-04	27.5	9.1	12.58	104.31	
FD3-15S	300	1.50	73.3	1	5.683E-03	5.011E-04	23.7	13.6	12.58	127.54	Modified Data
FD3-2	300	2.00	55.0	1	6.473E-03	5.011E-04	21.6	18.2	12.58	146.98	Modified Data

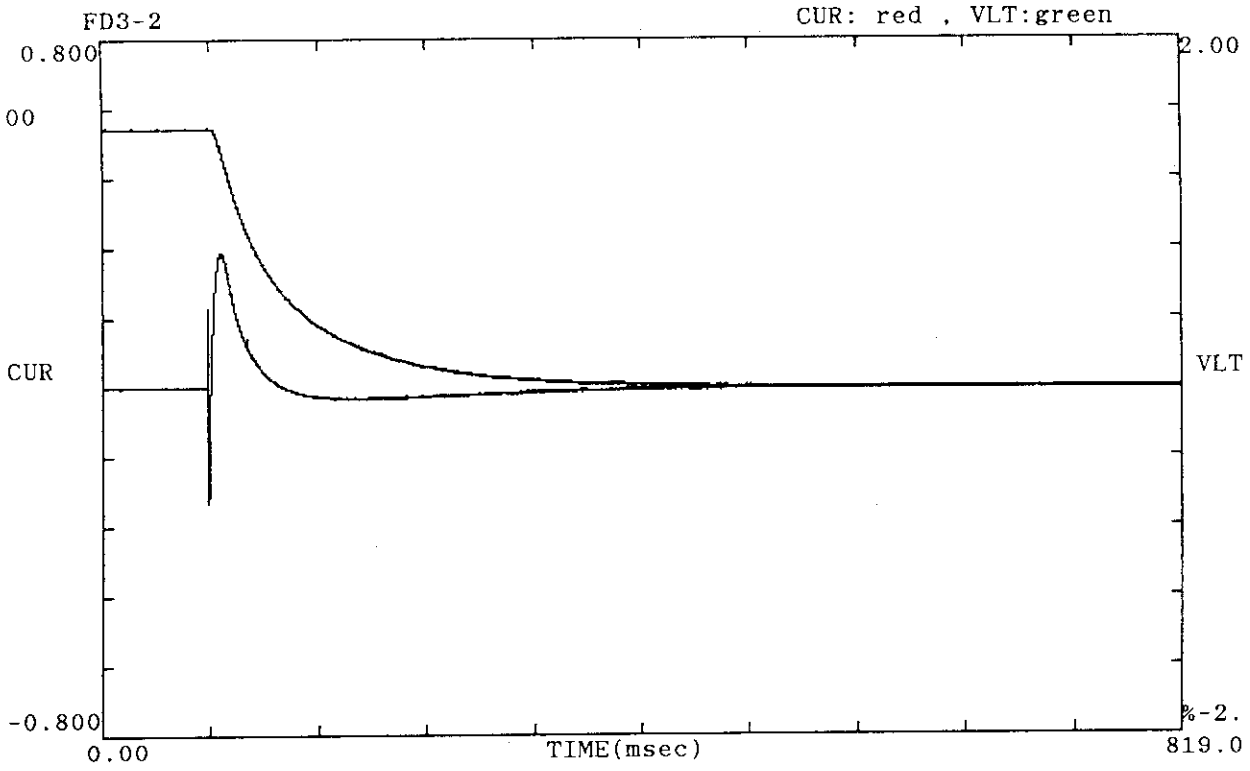
FD3-2
CUR: red , VLT:green
0.800
00
CUR
-0.800
0.00
TIME(msec)
2.00
VLT
%-2.
819.0

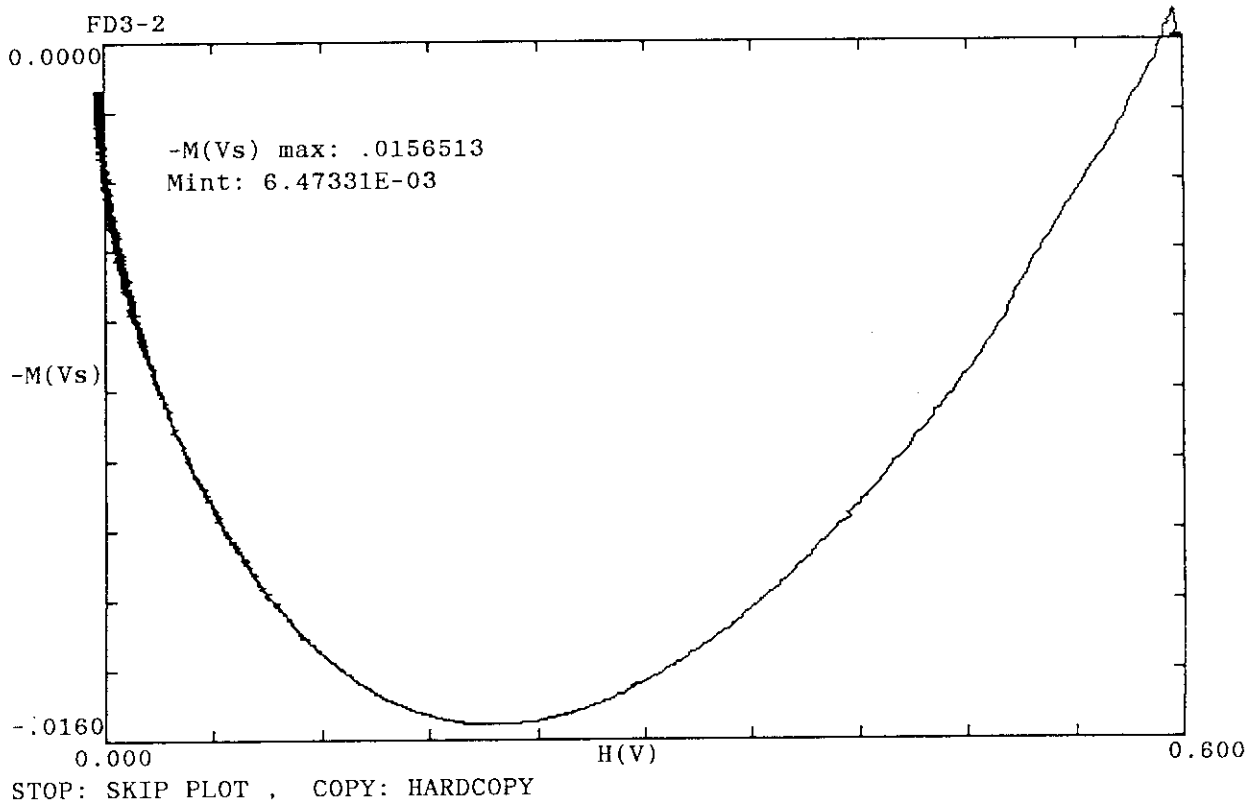
FD3-2
0.0000
-M(Vs) max: .0156513
Mint: 6.47331E-03
-M(Vs)
-.0160
0.000
H(V)
0.600
STOP: SKIP PLOT , COPY: HARDCOPY

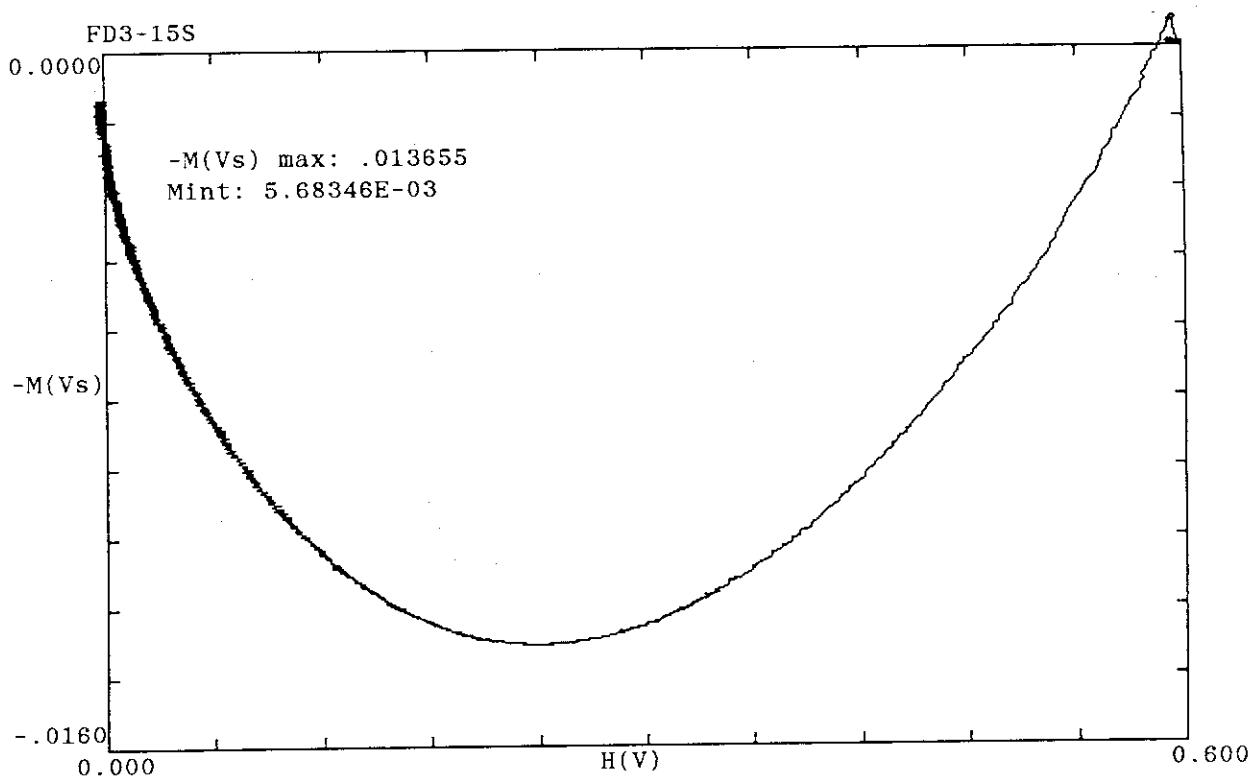

STOP: SKIP PLOT , COPY: HARDCOPY

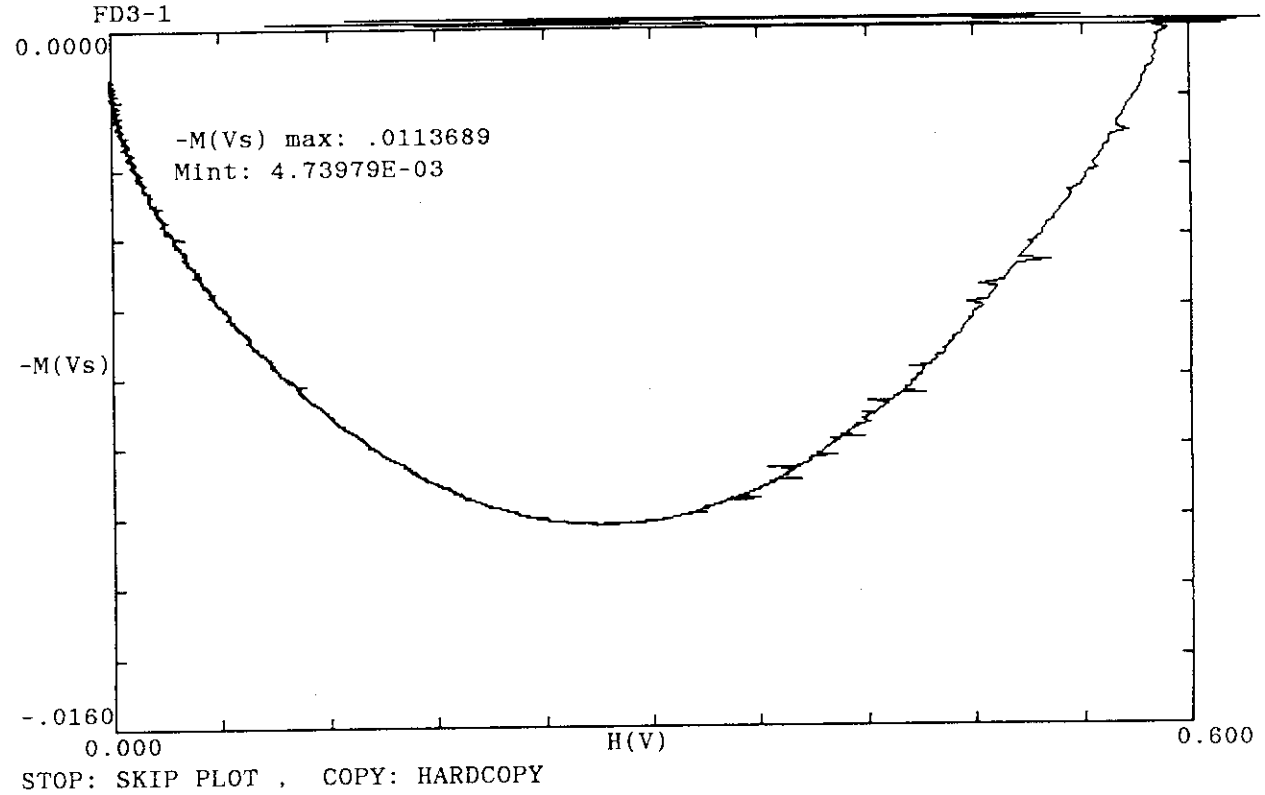

STOP: SKIP PLOT , COPY: HARDCOPY

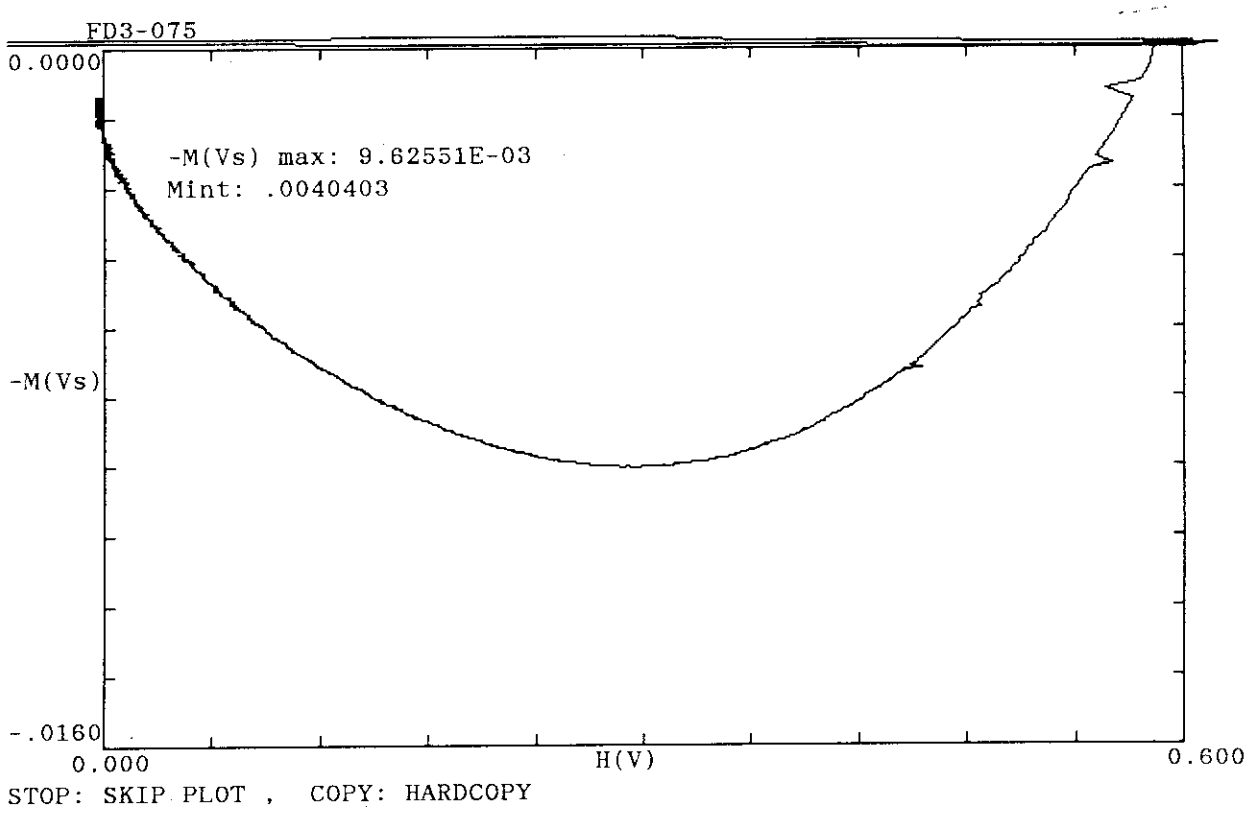
FD3-075
0.0000
-M(Vs) max: 9.62551E-03
Mint: .0040403
-M(Vs)
-.0160
0.000
H(V)
0.600
STOP: SKIP PLOT , COPY: HARDCOPY

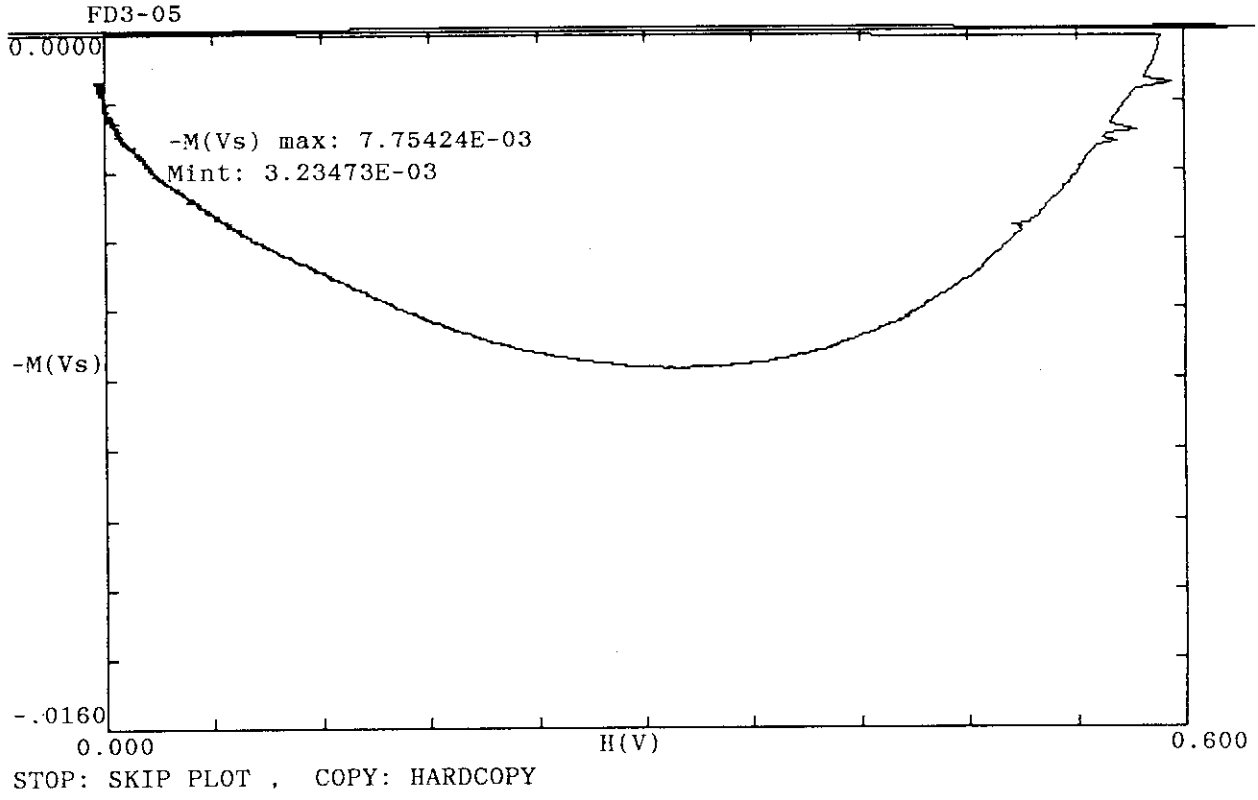
FD3-05
0.0000
-M(Vs) max: 7.75424E-03
Mint: 3.23473E-03
-M(Vs)
-.0160
0.000
H(V)
0.600
STOP: SKIP PLOT , COPY: HARDCOPY

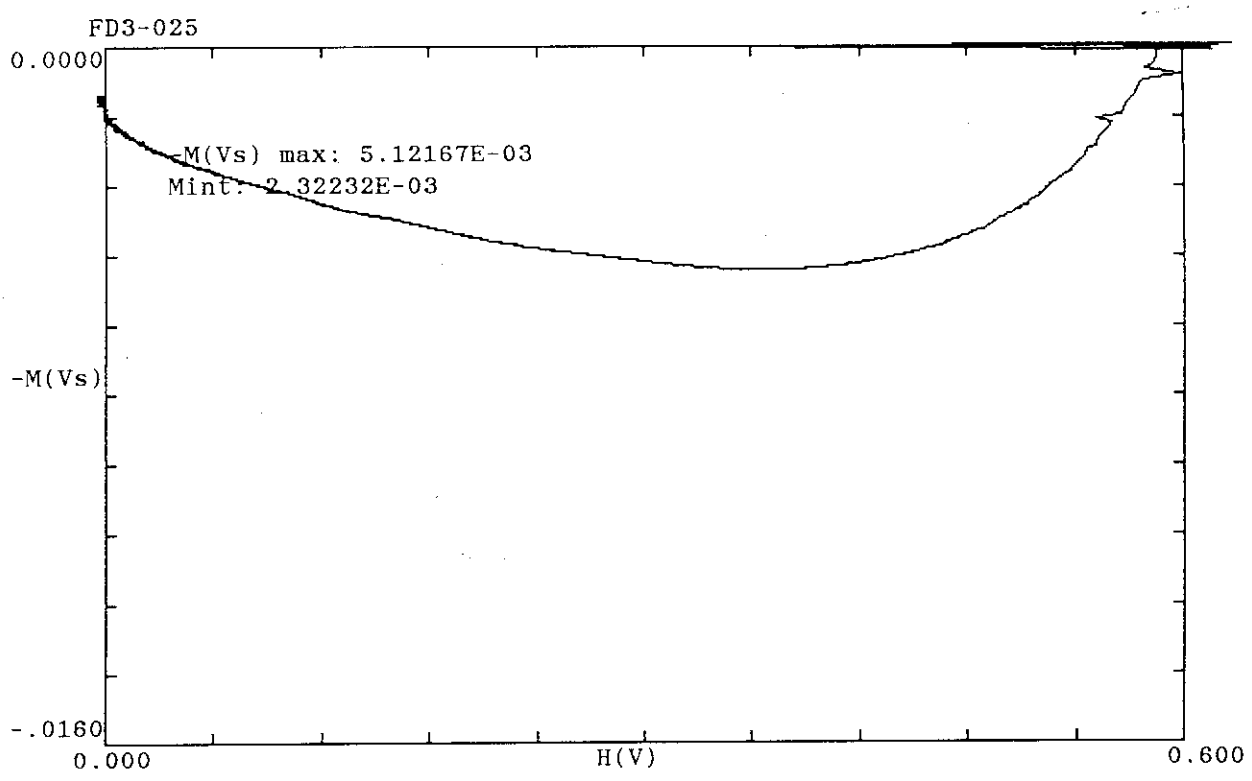

STOP: SKIP PLOT , COPY: HARDCOPY

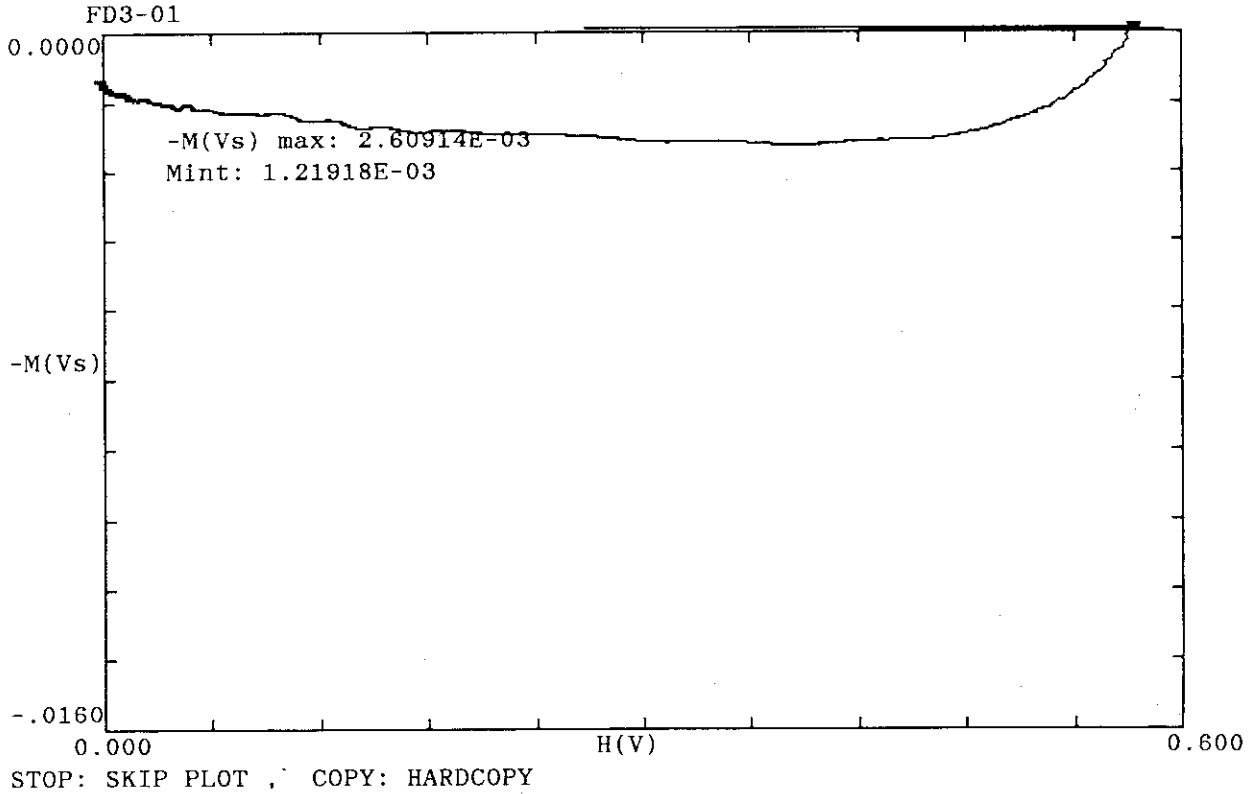

STOP: SKIP PLOT , COPY: HARDCOPY

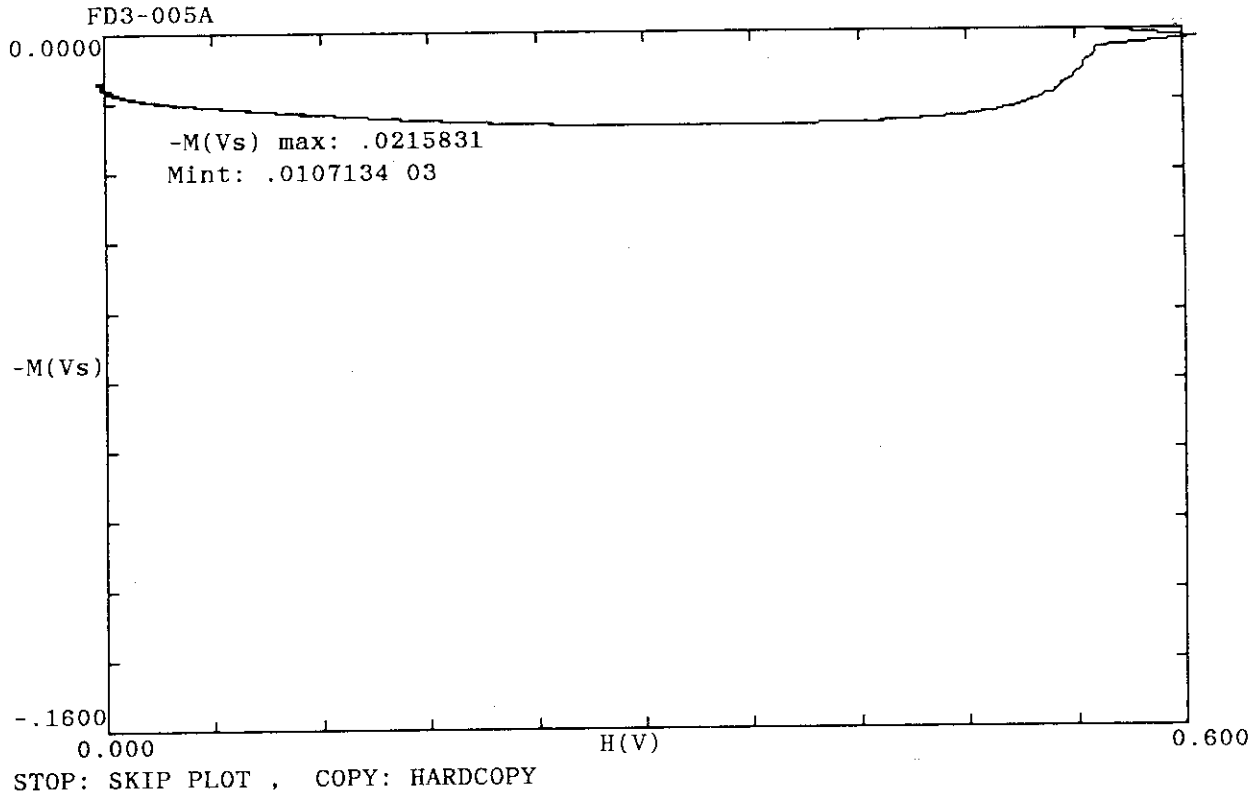

Furukawa Sample

Exponential Dump through a 2 Ω Resistor

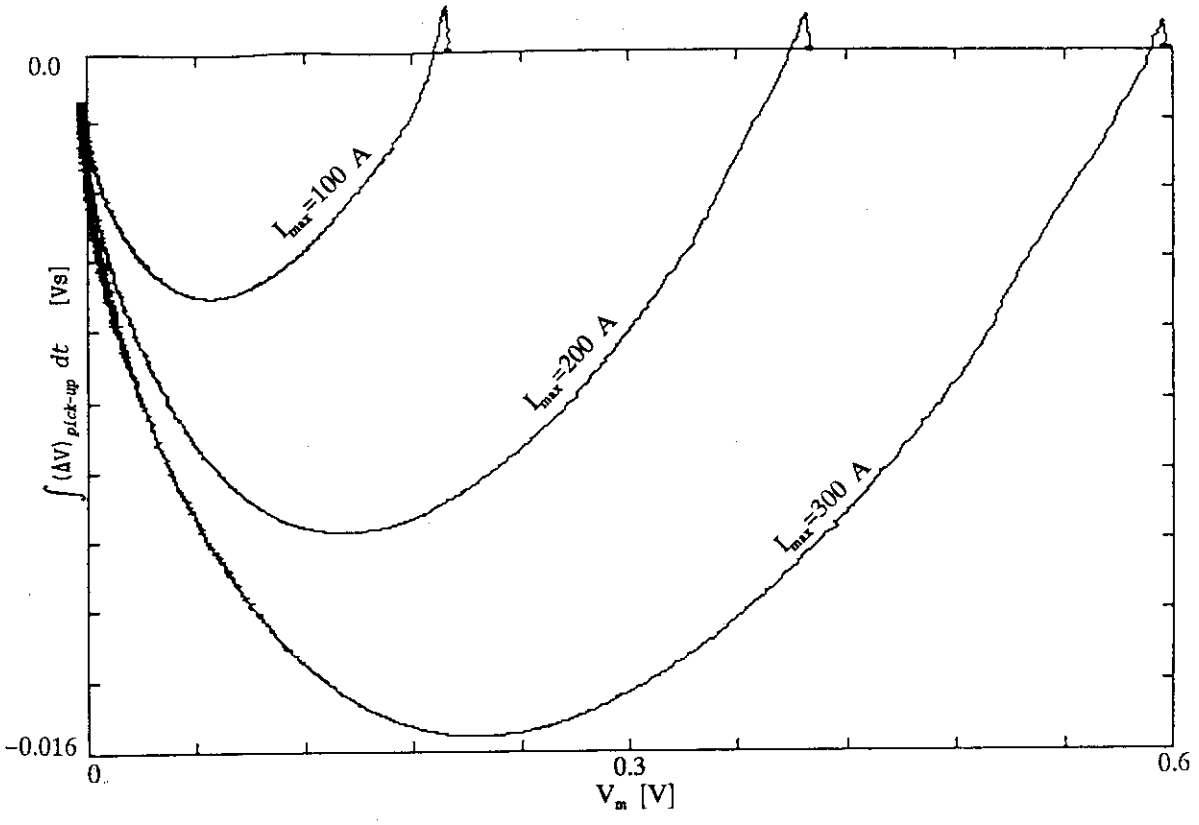

A.C. Loss Data and Analysis (experiment date: June 16-18, 1993)
Hitachi Data

File Name	Imax (A)	Rdump (ohm)	t (ms)	Ampl. (x)	Mint (V^2•s)	Ahys† (V^2•s)	tcpl (ms)	1/t (1/s)	Qhys (mJ/cc)	Qcpl (mJ/cc)	Remark
HD1-01A	100	0.10	1100.0	10	1.775E-03	1.425E-03	25.0	0.9	4.23	1.29	Polarity Reversal
HD1-025	100	0.25	440.0	1	1.862E-04	1.425E-04	12.5	2.3	4.23	1.61	
HD1-05	100	0.50	220.0	1	2.069E-04	1.425E-04	9.4	4.5	4.23	2.37	Modified Data
HD1-075	100	0.75	146.7	1	2.360E-04	1.425E-04	9.3	6.8	4.23	3.44	Modified Data
HD1-1	100	1.00	110.0	1	2.779E-04	1.425E-04	10.3	9.1	4.23	4.98	Modified Data
HD-15	100	1.50	73.3	1	3.056E-04	1.425E-04	8.5	13.6	4.23	6.00	Modified Data; Polarity Reversal
HD1-2	100	2.00	55.0	1	3.415E-04	1.425E-04	8.0	18.2	4.23	7.32	Modified Data

File Name	Imax (A)	Rdump (ohm)	t (ms)	Ampl. (x)	Mint (V^2•s)	Ahys† (V^2•s)	tcpl (ms)	1/t (1/s)	Qhys (mJ/cc)	Qcpl (mJ/cc)	Remark
HD2-005A	200	0.05	2200.0	10	3.206E-03	2.667E-03	15.4	0.5	10.00	1.62	
HD2-01A	200	0.10	1100.0	10	4.000E-03	2.667E-03	22.0	0.9	10.00	4.54	
HD2-025	200	0.25	440.0	1	5.340E-04	2.667E-04	18.7	2.3	10.00	9.47	
HD2-05	200	0.50	220.0	1	6.917E-04	2.667E-04	15.5	4.5	10.00	15.27	Modified Data
HD2-1	200	1.00	110.0	1	8.882E-04	2.667E-04	11.8	9.1	10.00	22.50	Modified Data
HD2-15	200	1.50	73.3	1	1.060E-03	2.667E-04	10.4	13.6	10.00	28.81	Modified Data
HD2-2	200	2.00	55.0	1	1.174E-03	2.667E-04	9.1	18.2	10.00	33.01	Modified Data

File Name	Imax (A)	Rdump (ohm)	t (ms)	Ampl. (x)	Mint (V^2•s)	Ahyś† (V^2•s)	tcpl (ms)	1/t (1/s)	Qhys (mJ/cc)	Qcpl (mJ/cc)	Remark
HD3-005A	300	0.05	2200.0	10	5.260E-03	4.750E-03	7.9	0.5	19.86	1.88	
HD3-01A	300	0.10	1100.0	10	7.147E-03	4.750E-03	18.9	0.9	19.86	8.82	
HD3-025	300	0.25	440.0	1	9.188E-04	4.750E-04	14.2	2.3	19.86	16.33	
HD3-05	300	0.50	220.0	1	1.338E-03	4.750E-04	14.3	4.5	19.86	31.78	Modified Data
HD3-1	300	1.00	110.0	1	1.771E-03	4.750E-04	11.1	9.1	19.86	47.71	Modified Data
HD3-15	300	1.50	73.3	1	2.130E-03	4.750E-04	9.7	13.6	19.86	60.89	Modified Data
HD3-2	300	2.00	55.0	1	2.319E-03	4.750E-04	8.2	18.2	19.86	67.87	Modified Data

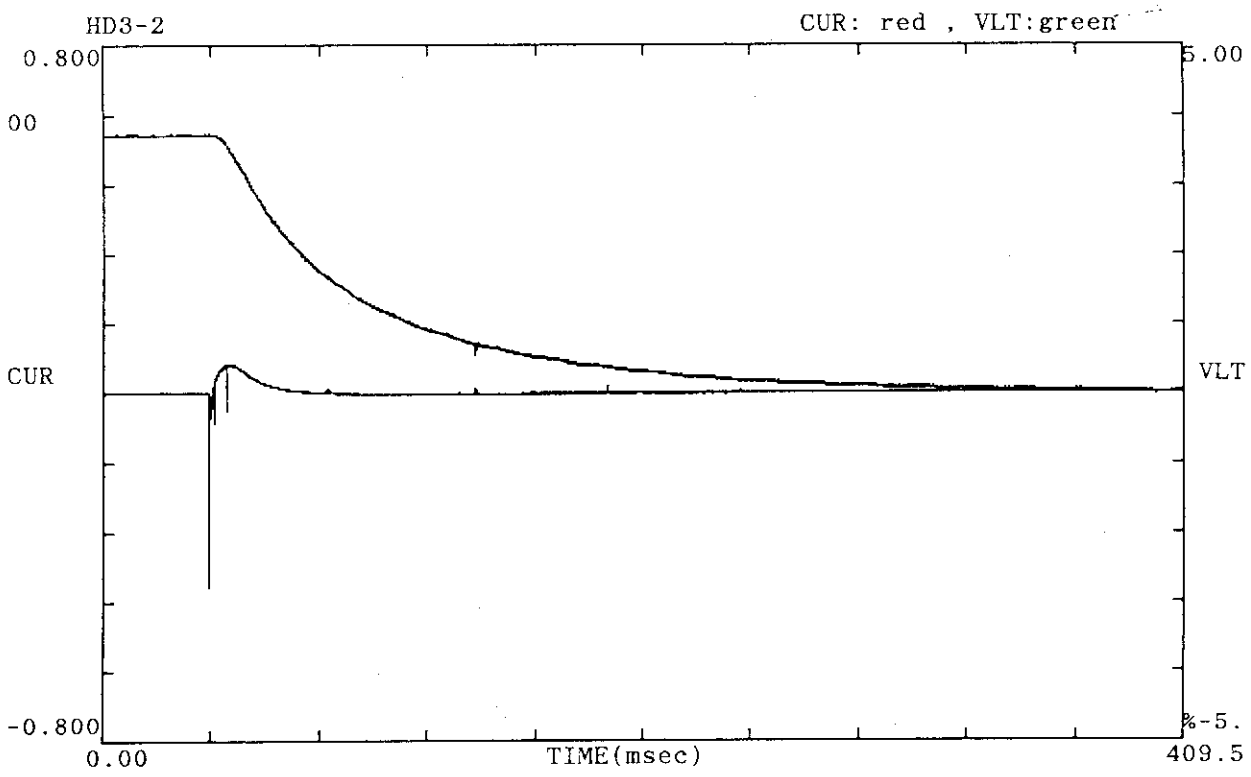

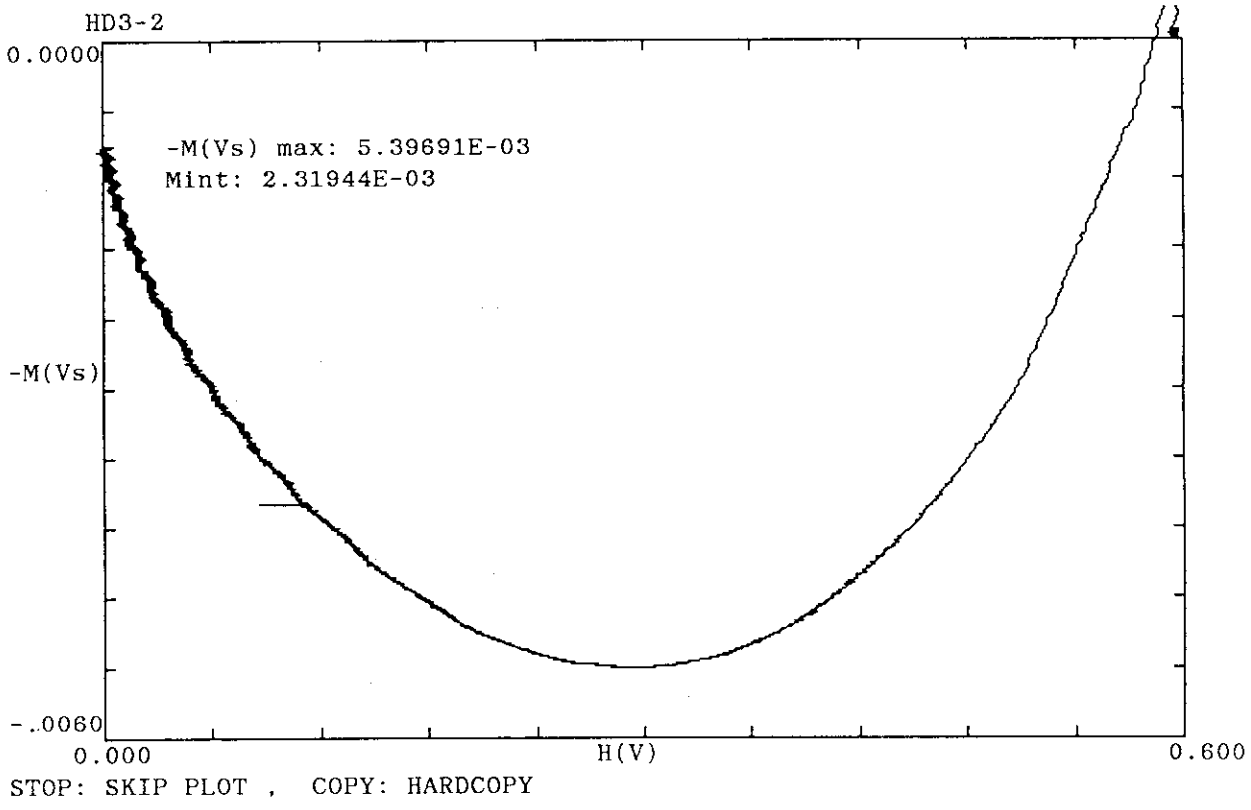

STOP: SKIP PLOT , COPY: HARDCOPY

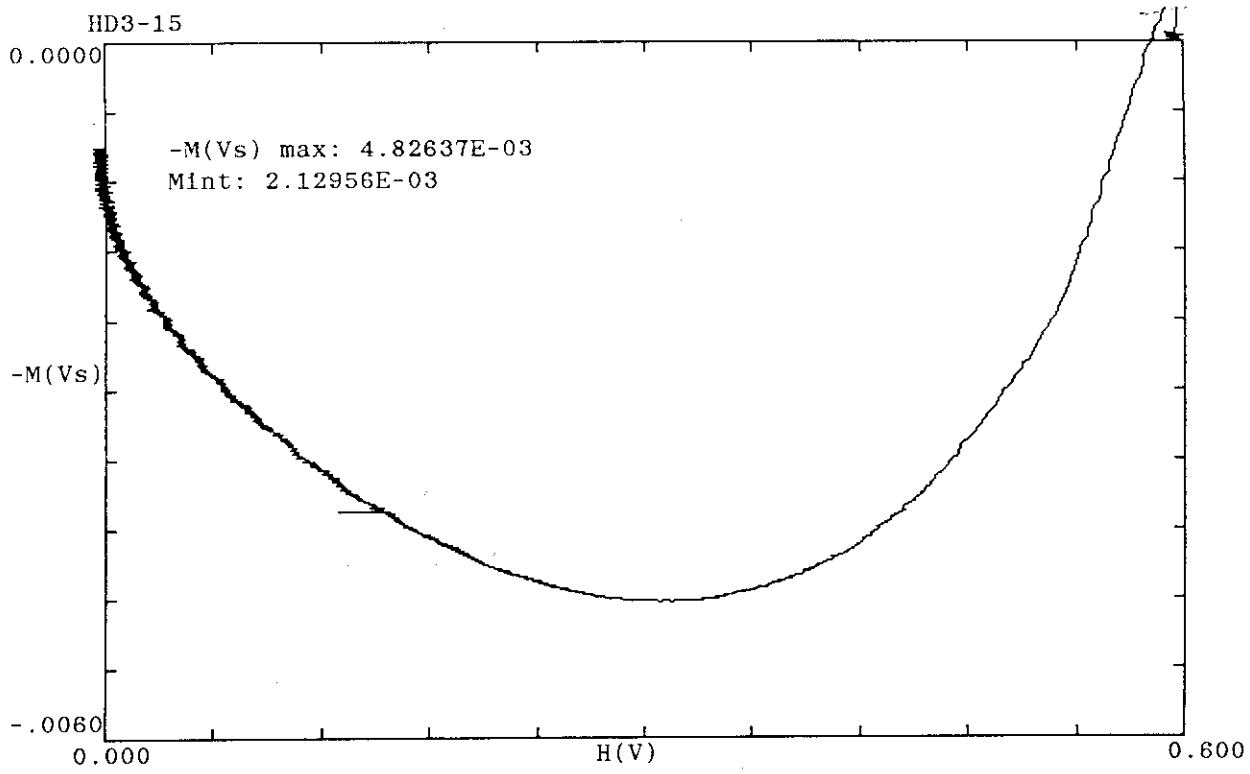

STOP: SKIP PLOT , COPY: HARDCOPY

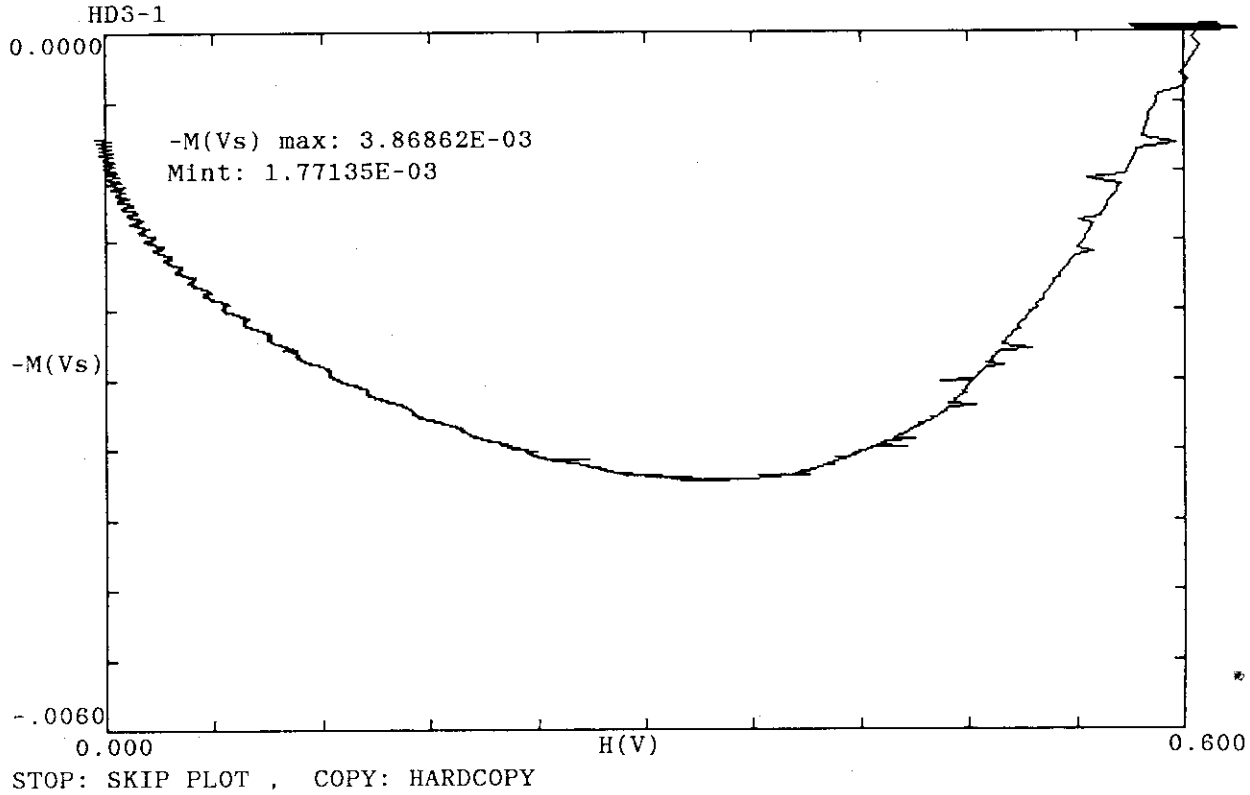

STOP: SKIP PLOT , COPY: HARDCOPY

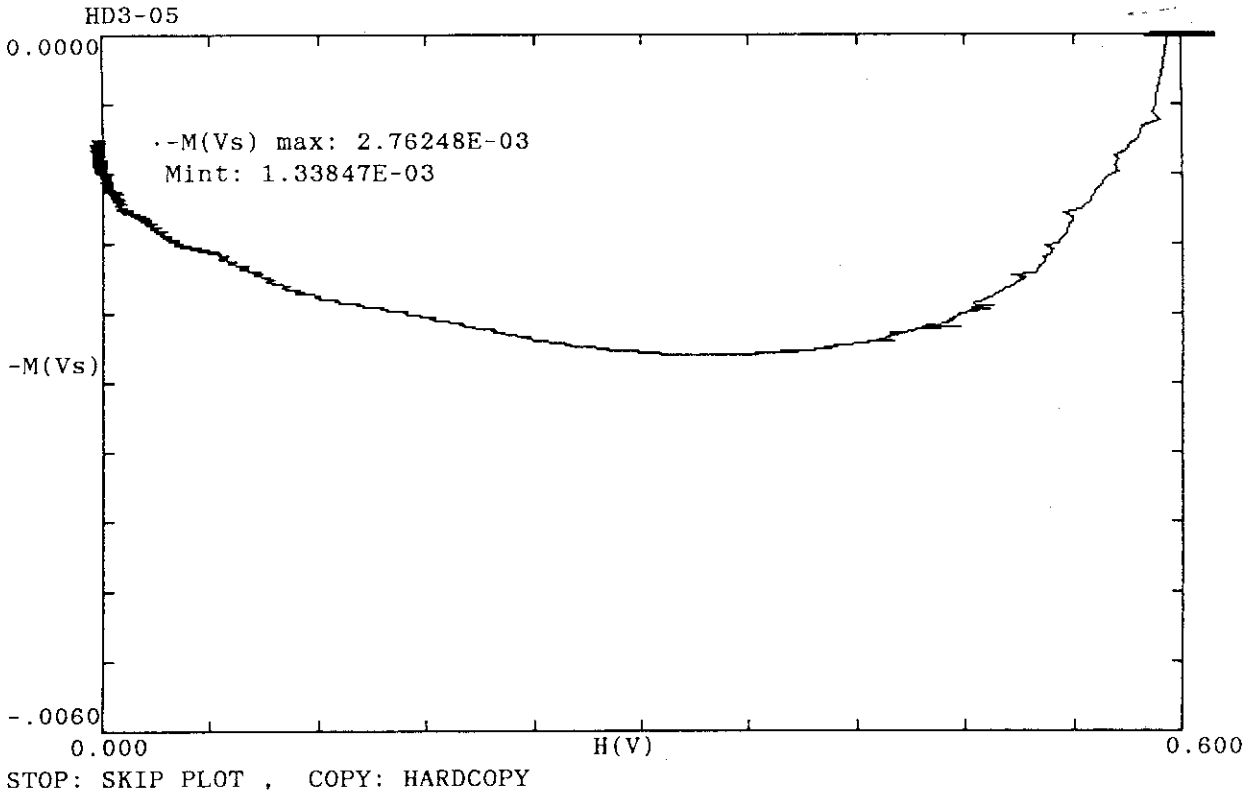
HD3-05
0.0000
-M(Vs) max: 2.76248E-03
Mint: 1.33847E-03
-M(Vs)
-.0060
0.000
H(V)
0.600
STOP: SKIP PLOT , COPY: HARDCOPY

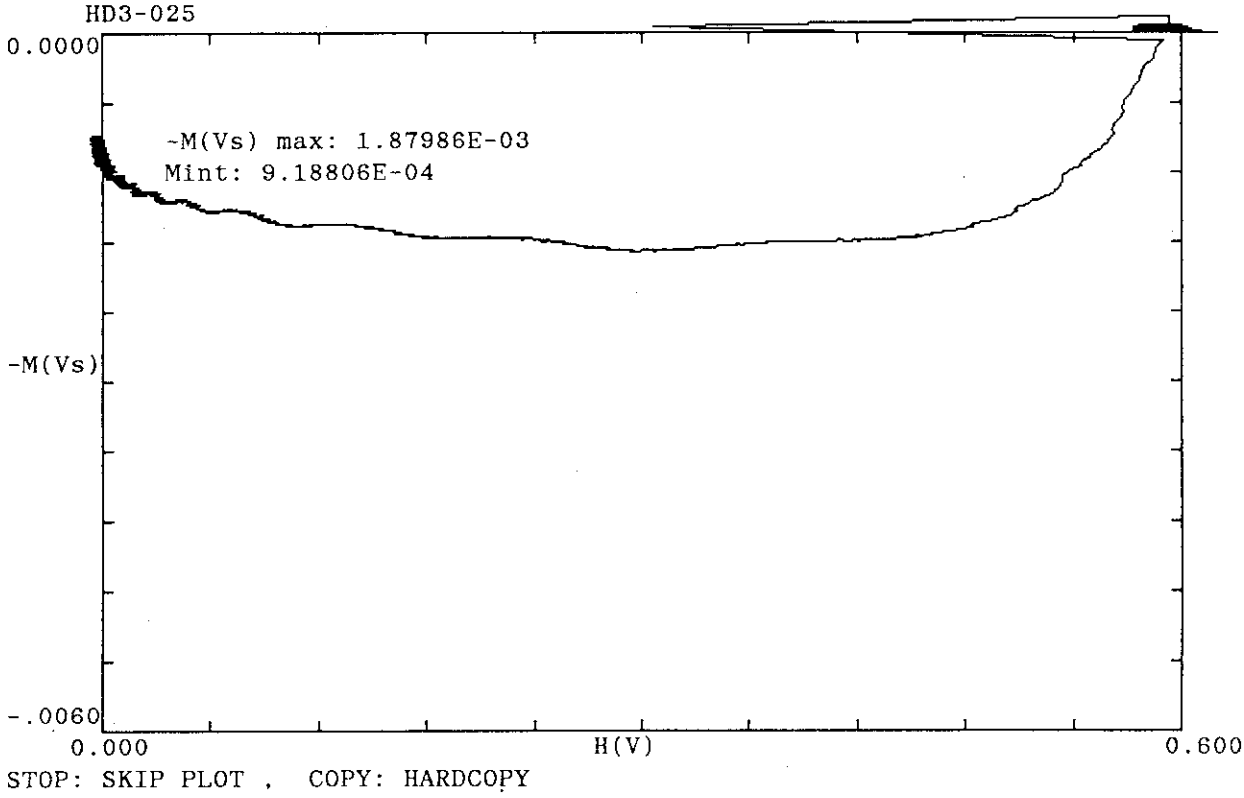
HD3-025
0.0000
-M(Vs) max: 1.87986E-03
Mint: 9.18806E-04
-M(Vs)
-.0060
0.000
H(V)
0.600
STOP: SKIP PLOT , COPY: HARDCOPY

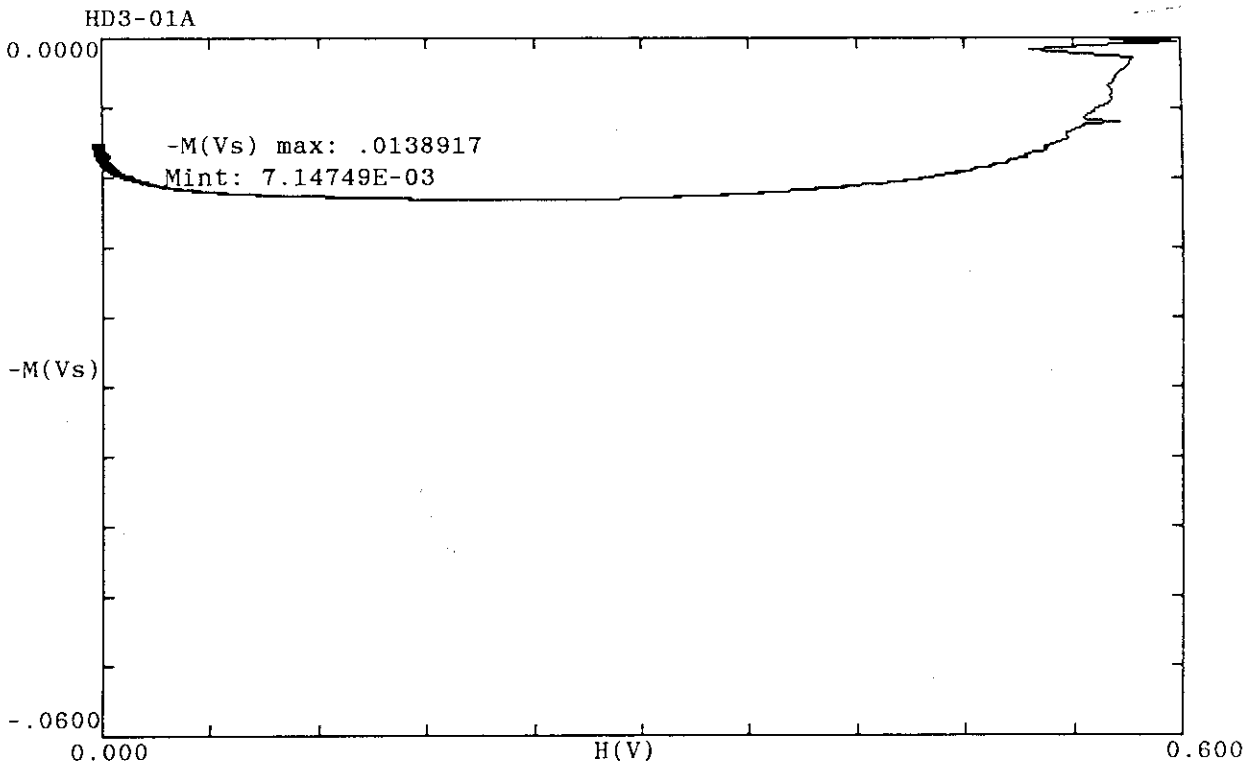

STOP: SKIP PLOT , COPY: HARDCOPY

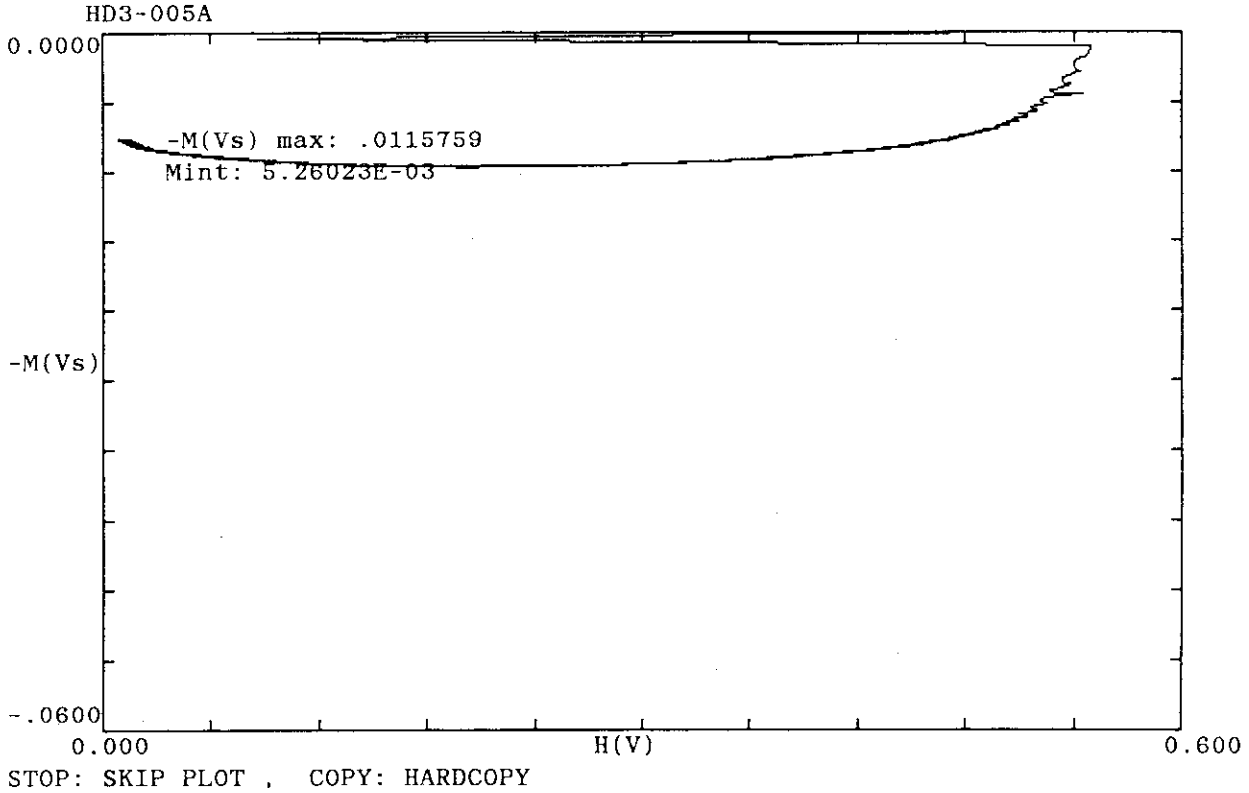

STOP: SKIP PLOT , COPY: HARDCOPY

Hitachi Sample

Exponential Dump through a 2 Ω Resistor